AMERICAN UNIVERSITY OF BEIRUT

DETECTION OF NICOTINE USING SURFACE ENHANCED RAMAN SPECTROSCOPY

by
MAIASSA MOUFID CHAAR

A thesis
submitted in partial fulfillment of the requirements
for the degree of Master of Science
to the Department of Chemistry
of the Faculty of Arts and Sciences
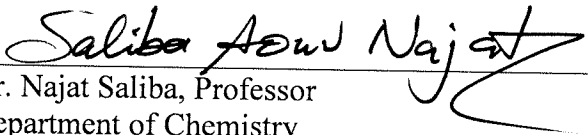at the American University of Beirut
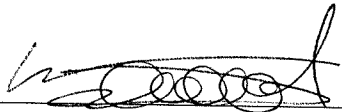
Beirut, Lebanon
January 2019
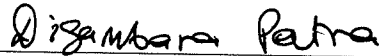
AMERICAN UNIVERSITY OF BEIRUT

DETECTION OF NICOTINE USING SURFACE ENHANCED RAMAN SPECTROSCOPY

by
MAIASSA MOUFID CHAAR

Approved by:

_____

Dr. Najat Saliba, Professor   Advisor
Department of Chemistry

_____

Dr. Walid Saad, Associate Professor   Co- Advisor
Department of Chemical and Petroleum Engineering

_____

Dr. Digambara Patra, Associate Professor   Member of Committee
Department of Chemistry

Date of thesis defense: January 22, 2019

iii

AMERICAN UNIVERSITY OF BEIRUT

THESIS, DISSERTATION, PROJECT RELEASE FORM

Student Name:
MOUFID   _CHAAR_   _MAIASSA_
                    Last   First
    Middle

⊗ Master's Thesis   ⭕ Master's Project   ⭕ Doctoral Dissertation

☐   I authorize the American University of Beirut to: (a) reproduce hard or electronic copies of my thesis, dissertation, or project; (b) include such copies in the archives and digital repositories of the University; and (c) make freely available such copies to third parties for research or educational purposes.

☒   I authorize the American University of Beirut, to: (a) reproduce hard or electronic copies of it; (b) include such copies in the archives and digital repositories of the University; and (c) make freely available such copies to third parties for research or educational purposes after:

> **One ---- year from the date of submission of my thesis, dissertation, or project.**
> **Two ---- years from the date of submission of my thesis, dissertation, or project.**
> **Three ✗ years from the date of submission of my thesis, dissertation, or project.**

Maiassa Chaar ·   _04/02/2019_

Signature   Date

This form is signed when submitting the thesis, dissertation, or project to the University Libraries

ACKNOWLEDGMENTS

I would like to like to express my sincere gratitude to my advisor Dr. Najat A. Saliba, for her constant help, support, and motivation throughout my masters. She consistently provided constructive feedback which made this thesis possible.

I would like to thank Dr. Walid Saad for co-advising this project and give valuable input to develop of this project. I would also like to thank Dr. Digambara Patra for his valuable feedback and for being part of my committee.

I want to express my appreciation to Dr. Ahmad El-Hellani for his tremendous help in this dissertation. I am thankful for the assistance and support of the research group, Rachel El-Hage, Lamis Al Aaraj and Salwa Hajjir. I want to express my appreciation to Ryan Gharios, for his fundamental help with experiments and theoretical discussions related to this project.

Finally, I would like to thank my family and friends for believing in me and for giving me that extra push.

AN ABSTRACT OF THE THESIS OF

Maiassa Moufid Chaar   for   Master of Science
<u>Major</u>: Chemistry

Title: Detection of Nicotine using Surface Enhanced Raman Spectroscopy

It has been established that smoking is highly associated with the development of serious medical problems. Clinical research has become essential to study not only exposure to toxicants but also to establish new products' regulations. Clinical study designs often require refrain from use of nicotine delivery product prior to the trial in order to homogenize nicotine levels in all participants and also to evaluate nicotine withdrawal symptoms. Typically, refrain from nicotine products is confirmed by the well-established breath carbon monoxide (CO) test. Nevertheless, CO test cannot detect the abstinence from using non-combustible tobacco products, such as Electronic Cigarettes (ECIG).

There is a demand to develop a method to fulfil the clinical need to selectively assess nicotine intake. Previous methods for detection of nicotine included High Performance Liquid Chromatography (HPLC) and Gas chromatography (GC), but these are time consuming and costly. Recently, Surface Enhanced Raman spectroscopy (SERS) emerged as a potential technique providing a simple, rapid and low-cost method.

In this study, SERS will be used as an alternative method to detect nicotine consumption. The ultimate aim of this project is to develop an analytical method able to detect low concentrations of nicotine in biological matrices, such as saliva or urine. To achieve that, a systematic study was conducted to develop surface enhancement consisting of nicotine adsorbed on stable nanoparticles. Initially, synthesis of silver nanoparticles was investigated, taking into consideration the reduction reagent, temperature, preparation time and stirring rate. Following, the enhancement of the nicotine detection was optimized by selecting the mixing techniques (Vortex Multi-Inlet Vortex Mixer (MIVM)) and the medium condition (mainly pH and salt concentration). The method was developed to quantify nicotine in urine samples, demonstrating an innovative way to detect nicotine in biological matrices at low concentrations.

CONTENTS

ILLUSTRATIONS

TABLES

CHAPTER I

INTRODUCTION

A. Smoking and nicotine detection

1. Smoking epidemic and electronic nicotine delivery system (ENDS)

Tobacco use is increasingly recognized worldwide as a serious public health concern.[1] In 2015, the World Health Organization (WHO) announced that tobacco use is directly correlated with the death of about six million people in the world each year, with 10% of these cases from second-hand smoke.[2] Smoking is commonly correlated with several diseases, such as coronary heart disease (CHD), chronic obstructive pulmonary disease (COPD), aortic aneurysm, and cancer.[3-4]

Historically, several approaches were undertaken to fight the smoking epidemic, including smoking cessation tools like nicotine replacement therapy (NRT) or harm reduction approaches like low-toxicant cigarettes (light cigarettes) and recently, modified tobacco products like electronic nicotine delivery system (ENDS). Electronic cigarettes (e-cigarettes), the most common prototype of ENDS, have gained popularity among tobacco users since their introduction into the market.[5-7] A study from the Center for Disease Control and Prevention (CDC) and the National Youth Tobacco Survey showed that e-cigarette use increased tenfold between 2011 and 2015.[8] However, surveys show that e-cigarette users may not be aware that their liquids contain nicotine. A survey conducted by The Truth Initiative Showed that 63%

of users of JUUL, a newly branded e-cigarette, did not know that this product contains nicotine.[9]

Previous studies suggested that e-cigarettes can completely replace tobacco cigarettes for smokers willing to quit smoking.[10-11] These devices are often promoted as safer alternatives to traditional combustible cigarettes, however the use of such products may increase the level of nicotine exposure and probably lead to addiction. Moreover, it has been reported that e-cigarette users are more likely to initiate use of combustible tobacco cigarettes.[6-7, 12] Unlike combustible cigarettes, e-cigarette vaporize a liquid of propylene glycol/glycerol, nicotine and other chemicals to produce an inhalable aerosol. This accounts for their safety since fewer degradation products are produced under their operating conditions. Nowadays, more than 400 brands and many designs of e-cigarettes exist in the market, but they all share the basic constituents: a rechargeable battery, a heating coil, a liquid reservoir and a mouthpiece (Figure 1).[13-14]

Figure 1. A) Different designs of e-cigarette. B) The main common compartments of e-cigarette.

2. Clinical studies

Clinical trials have become an important tool in evidence-based regulatory approaches of tobacco smoking because they allow us to understand smokers' behaviour, their exposure to toxicants and their withdrawal symptoms. Similarly, clinical trials are quite important in the nascent and booming research on e-cigarettes.[13, 15-16] Some studies revealed the acceptability of e-cigarette among smokers and their relation to abstinence from smoking.[13, 16] Understanding and evaluating the abstinence symptoms is instrumental for a successful smoking cessation

intervention. This is because the suppression of abstinence symptoms is extremely related to the acceptance of the alternative nicotine delivery device by the user. In theory, toxicant exposure reduction will be related with long-term decreased health risk, but if the device fails to suppress abstinence symptoms, this theoretical decreased risk is not probable due to device rejection by the smoker.[13]

Clinical studies design often requires patients to refrain from use of any nicotine delivery product prior to the trial, due to two main reasons: to investigate abstinence symptoms and to homogenize baseline nicotine levels in all participants at the beginning of the experiment. This step is important to ensure a low level of nicotine in all patients, enabling appropriate conclusions and correlations between nicotine delivery and time of use. The abstinence required changes from study to study, but it is often reported to be from 12 to 24 hours.[13, 16-17]

a. Refrain from smoking detection: carbon monoxide (CO) test

Currently, refrain from combustible tobacco products use is confirmed by the well-established exhaled breath carbon monoxide (CO) test.[18-19] Briefly the CO test measures CO in the exhaled alveolar breath using a user-friendly portable analyser. CO levels can also be determined in the blood as carboxyhemoglobin.[18] Nevertheless, CO tests cannot detect the abstinence from non-combustible tobacco products, such as smokeless tobacco products or e-cigarettes. Consequently, methods that can detect nicotine exposure from all tobacco products are definitely needed.

b. Refrain from smoking detection: HPLC and GC methods

Other ways of assessing participants' refrain from nicotine before clinical trial rely on the quantification of nicotine concentrations by gas chromatography (GC) or high-performance liquid chromatography (HPLC).[20-22] These methods when applied to measure nicotine levels in biological fluids (blood, saliva or urine) require several steps: sample pre-treatment, optimization of separation conditions, quantitation, and method validation. These methods are accurate and well-established, however they are time-consuming (for both sample preparation and analysis of the results), accordingly not appropriate for rapid testing. In addition, chromatography techniques required robust and expensive machines and use of costly high purity solvents.

c. Refrain from smoking detection: Alternative methods

Recently, researchers have shown increasing interest in techniques that are specific and sensitive enough to identify and quantify an analyte of interest with minimum requirements of sample preparation. Another important aspect that should be considered is the cost of the method employed. Development of nicotine detection methods have lately focus largely on molecularly imprinted polymers (MIP),[23-25] immunoassay,[26-27] and surface-enhanced Raman scattering (SERS) techniques,[28-30] as a result of their potential in providing simple and low-cost methods for nicotine.

Molecularly imprinted polymers (MIP) is a technique that uses a polymer with cavities that can interact selectivity with a chosen "template" molecule in order to be

detected. Several different sensor platforms can be used to detect the analyte, such as heat-transfer resistance and quartz crystal microbalance.[23, 25] Previous studies have reported that MIP could achieve a limit of detection suitable for this study, however the preparation of the template could be time consuming.[23, 25] Moreover, the formation of the template could be problematic. Studies have reported limitations such as irregular materials shape, poor site accessibility, incomplete templates removal and low binding capacity.[31]

On the other hand, immunoassay technique has been commonly used in bioanalytical detection, by making use of a specific antibody-antigen reaction. The antigen to be quantified is the analyte.[32] There are many types of immunoassay system in which different detectors are applied, such as enzyme immunoassay (EIA), radioimmunoassay (RIA), fluoroimmunoassay (FIA), chemiluminescent immunoassay (CLIA) and counting immunoassay (CIA). These methods have been reported for nicotine detection, with a low limit of detection, however it measures cotinine equivalents, not providing specificity for nicotine analyte.[26, 33]

Table 1 shows a comparison of nicotine detection methods highlighting the cost, sample preparation, acquisition time, selectivity and limit of detection differences among these methods. As mentioned before, HPLC and GC are limited techniques since they are time consuming and costly. In addition, it could also be mentioned that chromatography is a labour-intensive method which requires a specialized technician to analyze the results. Although MIP and immunoassay have

6

reported low limit of detection for nicotine analysis, they also include significant drawbacks. MIP was discarded since complications was reported in the fabrication of template. In addition, due to limitations in selectivity immunoassay was also discarded, as mentioned previously.

Recently surface enhanced Raman spectroscopy (SERS) has emerged as a potential technique providing a simple, rapid and low-cost method for nicotine detection.[34-35] In brief, SERS intensifies Raman signals coming from molecules of the analyte (nicotine) by binding these molecules to the surface of nanoparticles, this results in enhancement of the electromagnetic field, and thus more sensitivity. This method has been successfully used for the quantitative analysis of nicotine and its major metabolites and low limit of detection has been achieved as shown in Table 1. SERS was shown to be suitable for differentiating smokers than non- smokers.

Table 1: Comparison between commonly used nicotine detection techniques.

Method	Cost	Sample preparation	Acquisition time	Selectivity	Limit of detection (µg/ml)
HPLC	Expensive machines high cost of analysing the samples	Time consuming, several preparation steps	Time consuming, hours	Selective and specific	0.01[20-21]
GC	Expensive machines high cost of analysing the samples	Time consuming, several preparation steps	Time consuming, hours	Selective and specific	0.5[22]
MIP	Relative (Depend on sensor platform)	Time consuming, creation of a template	Depend of sensor platform	Selective and specific	0.01[23], 1.7[24], 6.5[25].

Immunoassay	Low cost	Time consuming, incubation	Fast	Measures cotinine equivalents	0.002[26], 0.07[27].
SERS	Low cost method with portable machines	Depend on clean up method	Fast, seconds	Selective and specific	0.1[28], 0.01[29], 0.08[30].

3. Metabolism of nicotine and smokers' level

There are many pathways of nicotine metabolism in the human body, leading to six primary metabolites. Cotinine metabolite is the most abundant considering that about 70– 80% of nicotine is converted to cotinine.[36]

This study focused on the analysis of nicotine, since its availability and half-life are adequate to analyse refrain from nicotine intake 12 hours before a clinical trial. In other words, nicotine in the body has a half-life of about two hours and other metabolites with longer life-times are not appropriate to test refrain of few hours. The selection of a technique suitable for determining the presence of nicotine in bodily saliva or urine depends on the expected concentration of nicotine. Figure 2 shows nicotine and cotinine levels in biological samples detected in smokers after chewing 1 mg of nicotine.[37] It is clearly noticed that the urine levels of nicotine are significantly higher than saliva (peaks of 1200 ng/mg in urine and 300 ng/ml in saliva). Another important aspect is that after around 5 hours the levels of nicotine in saliva are close to zero, while in urine the levels reach 400 ng/mg.
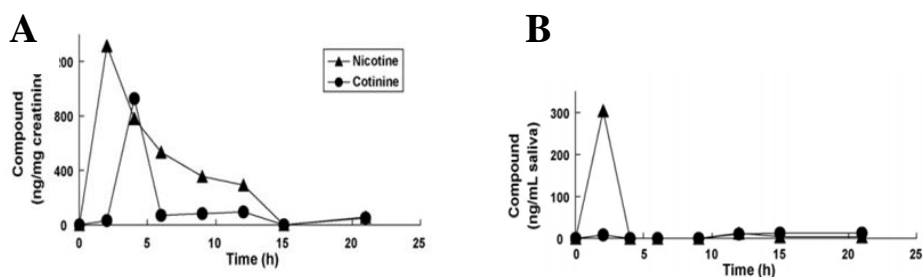
Figure 2. A) Nicotine and cotinine levels in urine(normalized by creatinine) and B) saliva after nicotine intake (1 mg of nicotine).[37]

Table 2 shows typical nicotine concentration in urine samples of smokers and non- smokers in µg/ml mentioned in different studies.

Table 2: Nicotine concentration in urine of smokers and non- smokers.

Urine non-smoker(µg/ml)	Urine smoker (µg/ml)	Comment
0.0075	1.35	GC method, 138 people.[38]
0.0083	1.75	GC method, 194 people.[39]
0	1.59	GC method, 344 people.[40]
0.002	1 to 5	HPLC, review.[41]

An adequate method to test refrain from nicotine must be able to differentiate smokers from non- smokers, with a detection limit around 1.5 µg/ml (1500 ng/mg) according to smokers level reported in Table 2. As shown before in to Table 1, SERS method could successfully reach this limit of detection.

B. Surface Enhanced Raman Spectroscopy

1. Vibration Spectroscopy: Raman and Infrared Spectroscopy

Vibrational spectroscopy comprises two analytical techniques: infrared (IR) and Raman spectroscopy. It is considered an extremely specific spectroscopic technique that enables detection of molecules through their particular molecular fingerprint, since it measures vibrational energy levels that are associated with chemical bonds of the molecule. The selection rules for Raman scattering and Infrared absorption are different, but the chemical information is similar, while a Raman active vibration should show a change in polarizability, IR active vibration should present a difference in dipole moment.[42]

Figure 3 shows an example of vibrational modes of a carbon dioxide (CO_2)

Symmetrical stretch

No change in dipole moment therefore IR inactive
There is change in polarisability therefore Raman active

Asymmetrical stretch

There is change in dipole moment therefore IR active but Raman inactive

In plane bending   Out of plane bending

The deformation vibrations of CO_2 are degenerate and appear at the same region (666 cm^{-1}) in the IR spectrum of CO_2. There is no change in polarisability therefore these vibrations are Raman inactive.

molecule. The IR and Raman active modes are indicated below each type of vibration.

Figure 3 - Example of vibrations of carbon dioxide (CO_2) molecule. As a rule of thumb, Raman active vibration should show a change in polarizability, IR active vibration should present a difference in dipole moment.[43-44]

Because of different selection rules, Raman and IR spectroscopy are considered complementary vibration studies of a molecule. While IR spectroscopy is an absorbance process, Raman scattering build upon emission from the sample, caused by irradiation from a laser. Figure 4 shows the difference between the spectroscopic transitions of Raman and IR Spectroscopy.
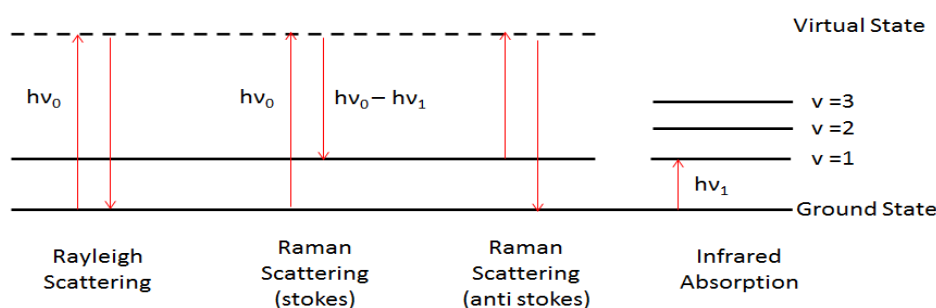
Figure 4 - Spectroscopic transitions of Raman and IR Spectroscopy. ν_0 indicates laser frequency, while ν_1 indicates vibrational quantum number. The virtual state is a short-lived distortion of the electron distribution by the electric field of the incident light. [45]

According to Figure 4, Raman spectroscopy involve vibration transition indirectly by light scattering. However, the Raman shift has the same energy as infrared absorption.[45] IR spectroscopy relies on absorption of matching frequency energy. The process in Raman is quite different than absorption, first the analyte undergoes excitation to a virtual state, and during relaxation the following processes can happen: the molecule can return to its original vibrational state (Rayleigh scattering), or it could go to a higher vibrational state (Stokes scattering) or a lower vibrational state (anti-Stokes). [42, 45-46]

11

Whilst both Infrared (IR) and Raman can offer the benefits of vibration spectroscopy, there are few fundamental differences that should be considered while applying both techniques. First, IR is very difficult to use in aqueous environments similar to that of biological fluids, whereas the Raman cross section of water is low, which makes Raman the technique of choice for analysis of samples dissolved in aqueous phase.[42, 45] Another fundamental difference between IR absorption and Raman scattering is probability, with absorption being a far more likely event. As an illustration, typically in IR the analyte absorbs around 90% of the incident light, but only about 1 in 10^{10} incident photons will undergo Raman Scattering.[35]

The discovery of Raman Scattering by Krishna and C.V. Raman occurred in 1928. They observed scattered radiation using a telescope focusing sunlight onto a sample of an organic liquid or vapour. In 1930, C.V. Raman was awarded the Nobel prize in physics for "his work on the scattering of light and for the discovery of the effect named after him".[47] Almost fifty years after the discovery of Raman spectroscopy, surface Enhanced Raman Spectroscopy (SERS) was first introduced in 1974 when Fleischmann et al reported a spectra of pyridine 106 times more enhanced than common Raman Spectroscopy on an electrochemically roughened silver electrode.[48] This was a breakthrough in the scientific community, making Raman Spectroscopy a powerful tool that now could be applied on aqueous matrices containing trace amounts of analytes, for example biological samples.

2. Surface Enhanced Raman Spectroscopy (SERS)

In a nutshell, the SERS effect is about intensifying Raman signals coming from molecules by several orders of magnitude.[35] The key factor for the powerful enhancement is the nanostructures present in the system. Two mechanisms contribute to the total enhancement: the electromagnetic and the chemical enhancement, which can both lead to the average of $10^4 - 10^6$ enhancement factors.[35, 45]

a. Electromagnetic Enhancement (EM)

The amplification of the signals in SERS comes mainly through the electromagnetic interaction of the laser light with metals, which produces large amplifications of the laser field through excitations generally known as plasmon resonances. Figure 5 shows a schematic illustration of the phenomenon. First, the incident laser irradiation hit the metal surface, exciting the surface plasmon on the metal. The excited surface plasmon consist of conductive oscillating metal electrons which enhances both the incident laser irradiation and the Raman scattering of the target analyte. For the enhancement to happen, the molecules must be adsorbed on the metal surface, or be very close to it (commonly≈10 nm). The electromagnetic enhancement is a main process for the SERS enhancement, and could reach up to 10^6 enhancement factor.[35, 49]
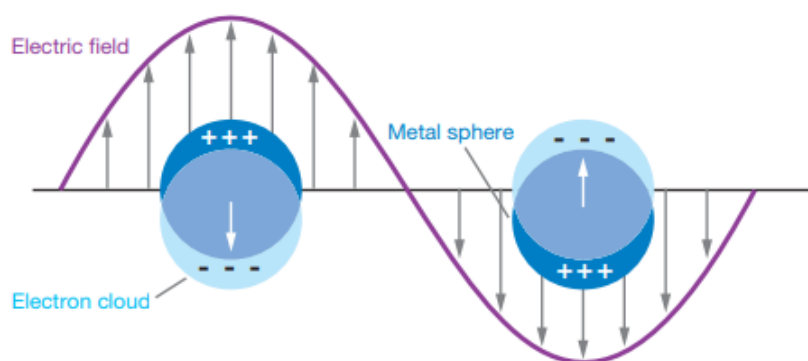
Figure 5. A surface plasmon is characterized as a surface charge density wave at a metal surface. The plasmons allows molecules close to the surface to intensity their spectra.[50]

b. Chemical enhancement (CM)

      The chemical mechanism requires strong interaction between the metal surface and the analytes through bonding. There is no clear explanation to this mechanism, however the most widely accepted is the so-called charge-transfer (CT) mechanism. The molecule must be chemically adsorbed on the surface and an electron from the metal will be transferred to the adsorbate. Therefore, a change in polarizability for certain vibrations will occur, which will lead to enhancement of the signal.[42]

3. *Substrates in SERS*

      SERS substrates are defined as any metallic structure (or nano-structure) that produces the SERS enhancement.[35] As a rule of thumb, great enhancements are successfully achieved if the substrate allows plasmon resonances (oscillation of conduction electrons). To achieve that, the structures are typically made of

14

metals, since they present the "right" optical properties. Furthermore, the substrate also must present dimensions in the sub-wavelength range, usually less than ~100 nm.[35, 49] Throughout the evolution of SERS, many substrates were developed based on such characteristics, achieving enhancement as high as 10^{10} .[35]

Substrates can be roughly classified into three main classes: metallic particles (typically nanoparticles) in solution, such as colloidal solutions, 'planar' metallic structures, which are arrays of metallic nanoparticles on a planar plate (metals, silicon, glass, etc) and metallic electrodes.

Solutions of metallic colloids predominantly made of silver (Ag) or gold (Au) have been widely used.[35] Their main advantages are simple preparation and high enhancement factors. In addition, metallic colloids are strongly present in several significant developments in SERS, such as the first claims of single-molecule SERS detection.[35] The chemical reduction of metal salts is the most commonly and simplest synthetic method for formation of metal nanoparticles.[51-52]

4. Colloid formation

Synthesis of nanoparticles usually requires a soluble metal salt, a reducing agent, and a stabilizing agent. The stabilizing agent caps the particle and prevents aggregation or further growth. Reducing agents such as sodium borohydride and sodium citrate are commonly used for the preparation of metal nanoparticles.[35, 52]

Reaction 1 and Figure 6 below illustrate the mechanism of formation of silver

nanoparticles, according to Lee and Meisel method.[53]

$$4Ag^+ + Na_3C_6H_5O_7 + 2H_2O \rightarrow 4Ag^0 + H_3C_6H_5O_7 + 3Na^+ + H^+ + O_2\uparrow$$ [54] (Reaction 1)

$$Ag^+ + e_{aq} \rightarrow Ag^0 \rightarrow (Ag)_2^+ \xrightarrow{\text{(citrate)}^-} [(Ag)_2^+\cdots(citrate)^-] \rightarrow \bigcirc$$

Citrate capped
nanocluster

$$\cdots\rightarrow \quad + n(Ag^+) \cdots\rightarrow \quad Ag^+ \quad Ag^+ \quad Ag^+ \quad Ag^+ \quad Ag^+ \cdots\rightarrow$$

Agglomeration & cluster growth $\longrightarrow$

Stabilized
cluster
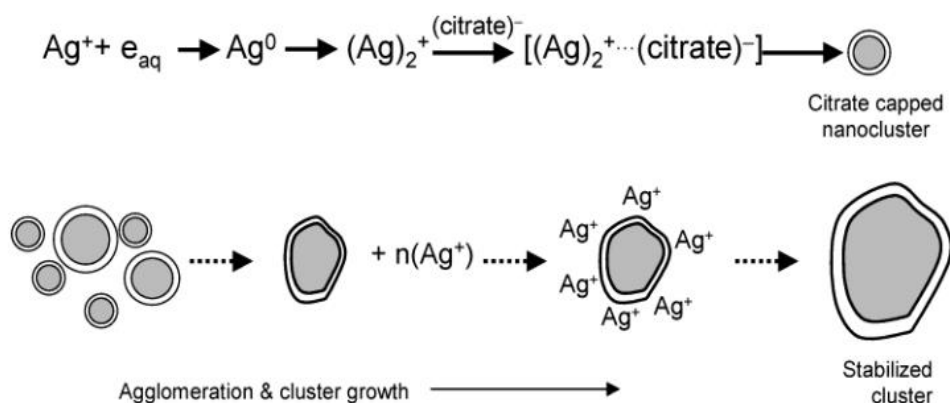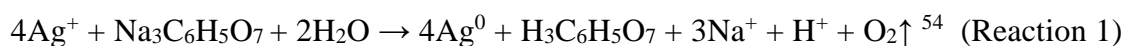
Figure 6. Primary and secondary growth steps in the formation of silver
nanoparticles.[51]

As shown in Figure 6, initially few seeds of silver particles are formed and

then create a strong complex with citrate anions. As the complex slowly grows by

further aggregation it reaches an optimal size. At this stage, there is a strong repelling

layer of citrate which prevents aggregation. Later, further grow happen though

Ostwald ripening, making larger particles grow at the expense of smaller ones.

Ostwald ripening is a theory that attribute the formation of colloids due to driving

forces arising from concentration of solute in the vicinity of small particles greater

than large particles, creating supersaturation.[55]At the bottom of Figure 6, smaller

particles are oxidized, thus Ag^+ ions re-adsorb on the larger silver particles going through reduction at the metal surface.[51] A significant amount of work has been dedicated in the literature on the understanding of the factors that control the size, shape, and polydispersity of the particles in these reactions.[35]

In this study, we investigated the potential of SERS in detecting refrain from nicotine intake prior to a clinical trial. Chapter two highlights the characteristics of the Raman machine used in this study and why it was chosen. Chapter three highlights the optimization of the nanoparticle formation by a citrate-reduction route, following Lee and Meisel method.[53] The synthesis of SERS substrate was optimized, including all the conditions that affect the formation of nanoparticles and thus affecting sample measurements. Chapter four shows the optimization of quantification of nicotine in urine matrix.

CHAPTER II

RAMAN SPECTROMETER

A. Introduction to Raman Spectrometer

Since the discovery of Raman effect in 1928, the technology of spectrometers has been evolving. Until the 50's, the signal was detected using photographic plate or a photomultiplier tube, and it was commonly reported issues such as intense fluorescence hiding Raman peaks and stray light.[56] In addition, samples needed to be extensively purified, and distillations commonly took months for preparation.[56-57] During the earliest period spectra were typically recorded with prism spectrographs and mercury lamps. The first commercial Raman instrument using dispersive gratings and laser as an excitation source, was introduced in 1966. In the 1970's, a microscope for Raman sampling was launched, which introduced many improvements, such as laser Focus, better signal collection and fluorescence rejection by the confocal optics.[57] After that, the use of Charge Coupled Device (CCD) detectors in 1980's contributed to a high acquisition speed of data. During the decade of 1990, manufacture of extended focal length led to a spectral resolution three times higher than previous instruments. Additionally, in this decade the first optical fiber coupled Raman probe was fabricated, contributing for the development of portable instruments.[56]

The optical design witnessed several improvements over the last 25 years, and innovations in terms of hardware and software.[58] Nowadays instruments with full

automation are commercially available. Moreover, portable instrumentation has rapidly expanded over the last decade and sample testing that once occurred in the laboratory is now executed in the field.[58]

In Raman spectroscopy, the laser source is focused onto the sample which enables scattering by the analyte to happen. The major compartments of a Raman spectrometer include a laser source to excite the molecule to the virtual level, optical, filters to select the Raman scattering, mirrors to conduce the light, and detector to capture the signal. Figure 7A represents the Raman probe, used for both excitation and collection of scattered light from the sample. Initially, the laser source is directed to the sample (green line to number 6). Next, light is emitted from the sample, and a portion of Raman scattered light is collected, while Rayleigh light is filtered (number 4). Filters are a very essential part in the instrument, since Rayleigh scattering is a dominant phenomenon, as mentioned previously in Chapter 1. The Raman component is then focused, and scattered photos will return from the same path moving toward the detector (red line). Figure 7B shows the portable instrument used in this study.
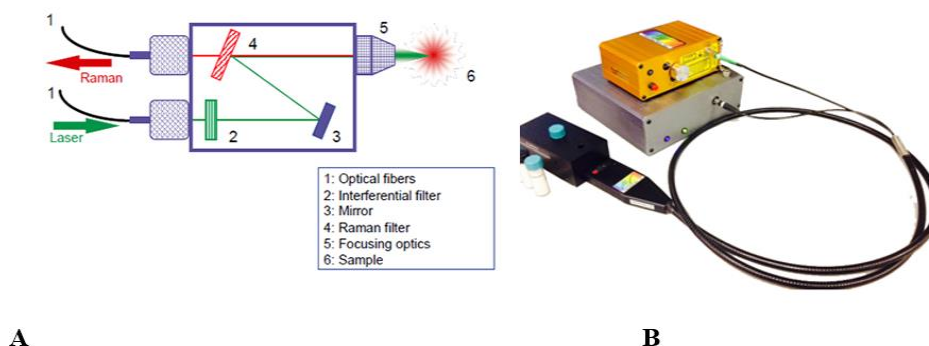
Figure 7. A) General scheme of a Raman Probe.[59] B) The portable Raman spectrometer 785 nm used in this study.

B. Raman Spectrometer: Selection and parameters

In general, in spectroscopy, when an analyte of a given concentration is analyzed on two similar instruments, the peak heights will be the same. Thus, assuming that we can correct for certain parameters, such as resolution, between different instruments, the peak height for that analyte must be the same. For example, if the same sample is scanned for longer times, the only difference will be better signal to noise ratio. Therefore, measuring a sample with UV/Vis or IR the peak height is independent of the measurement parameters, such as time of analysis.[60]

However, in Raman spectroscopy the measurement is different. The number of scattered photons is highly dependent on the machine. Therefore, the ordinate axis has arbitrary units (instead of %T units or absorption). Assuming that a sample is scanned for five times longer, the ordinate value (the peak height) will be five times higher in theory. Similarly, incident laser power affects the measurements. As a result, the peak

height in a Raman spectrum is not simply a function of the sample concentration, but also highly dependent on the measurement parameters (laser power, laser wavelength, scan times, orientation of sample, etc).[60]

In this study, initial experiments were done to understand and evaluate the effect of these parameters, since they are fundamental to ensure a successful detection. The most important factors to be considered while selecting a Raman system are sensitivity, which is affected by excitation wavelength, spectral range and resolution.[45] The choice of portability was based on versatility and cost balance, since recently portable devices has been employed due to a convenient, cost-effective, real-time, and on-site measurements.[61-62] In addition, clinical trials researchers are not chemists, thus there is a need to test nicotine on spot, to ensure refrain from tobacco product use. Then, portability of the instrument was considered due to is a real-time 'in situ ', user-friendly operation.

1. Effect of excitation wavelength

Excitation wavelength is one of the most important factors to consider when selecting a Raman spectrometer.[45] This is because laser wavelength extremely affects the measured spectra, as shown in Equation 1, below:

$$P_{Scattered} \propto \frac{I_o}{\lambda^4}$$

(Equation 1)

According to the Eq. (1), shorter wavelengths are more efficient and require less power than do lasers with longer wavelengths. Theoretically, a shorter wavelength will result in higher sensitivity, with $1/\lambda 4$ dependence.[45, 63] However, shorter wavelengths are also more likely to excite fluorescence due to more electric excitation that will occur in the ultraviolet (UV) and visible than the infrared region. Consequently, if a significant number of potentially fluorescence samples is anticipated, the laser wavelength should be as long as permitted by sensitivity requirements.[45] Auto-fluorescence has been reported as a major challenge in Raman spectroscopic analysis of organic and biological specimens.[64-65] Assuming that the excitation laser does not provide sufficient energy to the molecule, the required transition to achieve fluorescence will not occur. Nevertheless, if fluorescence occurs, it will be often much more intense than Raman scattering, hiding Raman peaks.[45, 66] To overcome this issue and diminish the probability of fluorescence, it has been suggested to select a system with longer laser wavelengths.[66]

We also selected adequate spectral range of 200-2750cm^{-1}, which includes the fingerprint area of nicotine. In addition, spectra resolution was also considered. This factor is important since it defines the minimum distance between two Raman peaks at which those peaks can both be distinctly observed. We selected spectra resolution of 4 cm^{-1}, since it was the best selectivity available for a portable instrument.

2. Effect of laser power and integration time

According to Equation 2 below, laser power is directly proportional to the number of scattered photons.[46]

$$I = Kl\alpha^2\omega^4$$

(Equation 2)

K is a constant derived from the speed of light, l is the laser power, ω is the frequency of incident radiation and α is the polarizability of the molecule. If you are not burning your sample or starting some photochemistry your laser power should scale linearly with the Raman signals.

3. Effect of position and cuvette

Background spectrum is defined as signal level that represents the expected output when a sample is not present. This is distinct from a dark spectrum, which is a set of counts versus wavelength values for a spectrometer at a given integration time when no light is present (either from the sample or from ambient environmental light sources). Both significantly influences the spectra.

It has been reported that quartz cuvettes provide lower interference of Raman signal compared to glass.[67] Since the portable instrument acquired was developed to accommodate glass vials, a customized quartz cuvette holder was built. The position

of the customized holder was carefully studied by placing the same sample at different positions using a millimetric paper, since angle and position of the sample is an important factor which affect the measurements, according to Equation 3, below.

$$I_s = I_0 \frac{8\pi\alpha^2 N}{\lambda^4 R^2} \sin^2(\theta)$$

(Equation 3)

Where I_s is the scatter efficiency of the laser, I_0 the incident light intensity, α is the polarizability of the molecular scatters, N is the number of scatters, R is the distance between the scatters and the observer, θ is the scattering angle, and λ is the wavelength of the incident light.

Figure 8 shows the customized quartz cuvette holder. To decrease the dark spectrum, a box was also fabricated to prevent light coming from the outside.
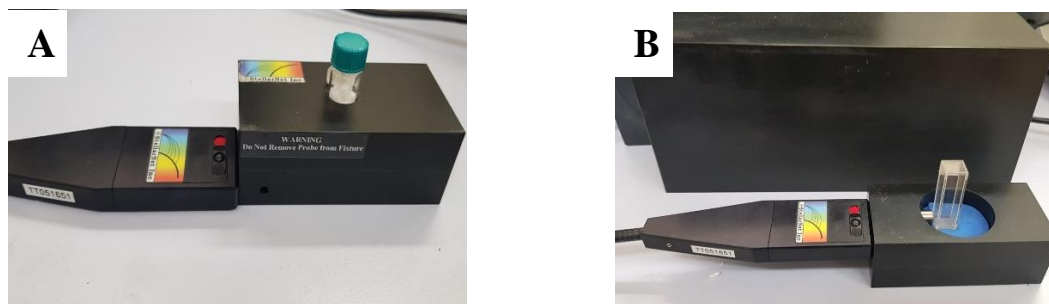
Figure 8. A) Original sample holder and borosilicate glass vial, B) Customized quartz cuvette holder and cover black box.

B. Results and Discussion

1. Effect of excitation wavelength

In order to check how excitation wavelength affects the measurements, we tested two lasers: 532nm and 785 nm. The effect of excitation wavelength is shown in Figure 9. We expected that the lower laser wavelength could generate more intense signals, according to Eq. 3. However, a laser wavelength of 532 nm proved to be inadequate for detecting nicotine samples, due to fluorescence (Figure 9A). Clearly, fluorescence caused a huge interference, overlapping and hiding Raman peaks. Figure 9B shows the collection of the same sample, in a system with a longer wavelength (785 nm). Indeed, our results are in accordance with the literature and fluorescence was successfully suppressed using longer wavelengths. Therefore, we decided to pursue the Raman system with 785 nm excitation wavelength.
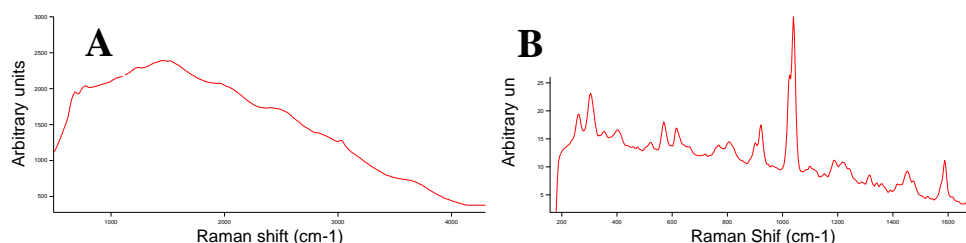
Figure 9. Pure nicotine spectra with different Raman instruments. A) 532nm excitation wavelength and B) 785 nm excitation wavelength Raman system.

2. Effect of laser power and collection time

After selecting the Raman spectrometer, parameters of the instrument were also optimized experimentally, to understand how they affect the final measurements.

Initial experiments focused on analysis of laser power and integration time. Laser power of our instrument varied from 1 to 8 (adjustable output of maximum 400mW). Collection time is simply the time that the detector will measure the scattered photons, thus by increasing collection time the signal will increase proportionally as discussed before. The collection time of the instrument has the interval from 1 to 30 seconds.

Figure 10A shows a collection of spectra of isopropanol at different powers. Isopropanol was used since this organic solvent is commonly used for the calibration of Raman systems.[68-69] In accordance with the theory, the maximum peak height achieved at maximum power (power 8, approximately 400mW). Figure 10b presents several spectra collected at fixed power 8, varying the collection time. As can be noticed, with an integration time of 30 seconds the peak height doubled.
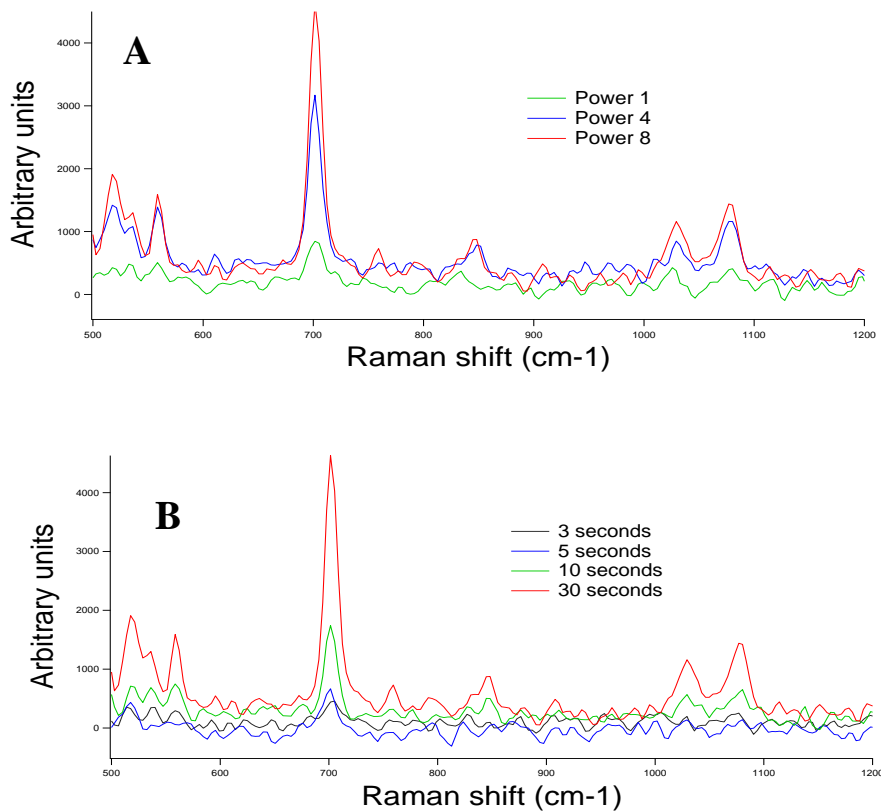
Figure 10. A) Effect of laser power on isopropanol solution, B) Effect of integration time.

Results confirmed that the glass vials contribute significantly to high interference in the background, we customized a sample holder to accommodate a quartz cuvette in the system originally fabricated for borosilicate glass (Figure 8). Figure 11A shows the difference in the background borosilicate glass vial and the quartz cuvette. Also, optimal position of the customized simple holder was evaluated, and the results are shown in figure 11B.

27
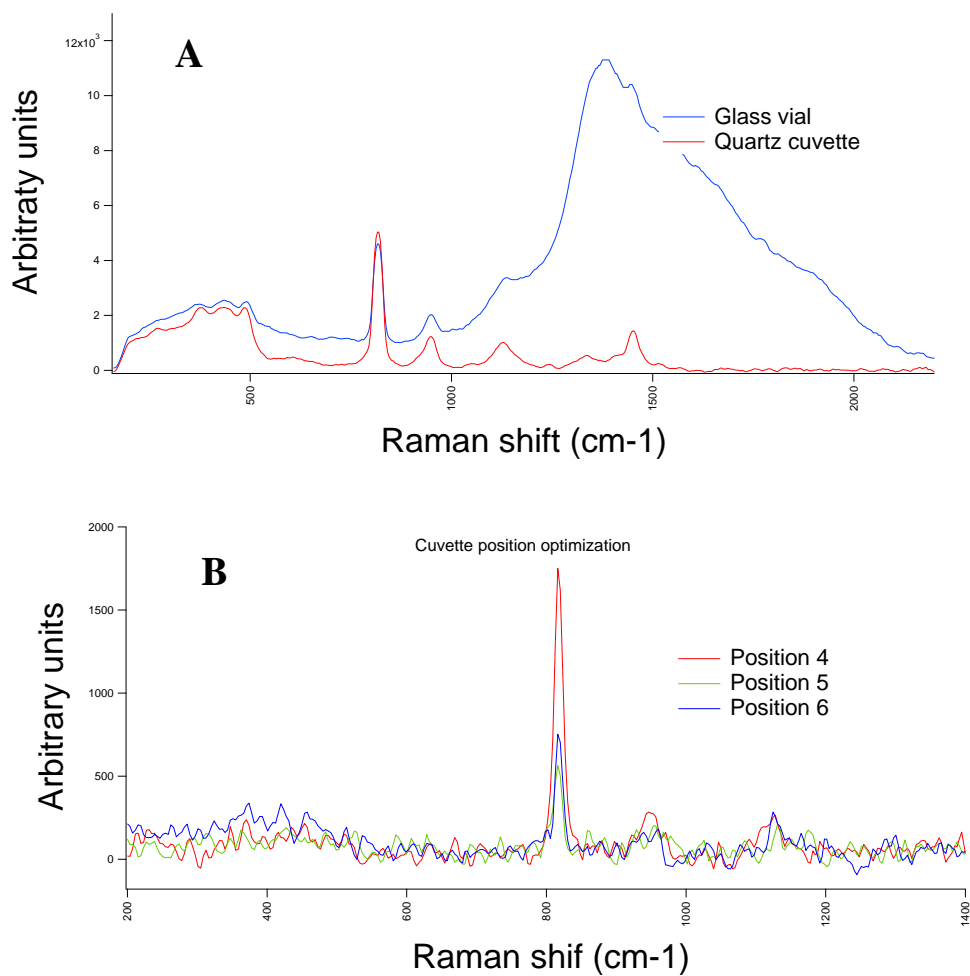
Figure 11. A) background reduction from quartz material in comparison with glass.
B) the study of the position of cuvette.

C. Conclusion

The importance of Raman parameters was demonstrated. Excitation wavelength is a crucial parameter to consider, especially if fluorescence coming from the analyte or matrices could hide the analytes' peaks, as seen in our study. Therefore,

by selecting a system with a laser source of longer wavelength (785 nm instead of 532 nm) this was overcome. Moreover, parameters of laser power and integration time were also demonstrated to significantly affect the measurements, duplicating the peak height in some cases. Furthermore, glass vials showed a significant interference in the spectra, and the system was adapted to accommodate quartz vials, that contribute to the removal of background considerably.

CHAPTER III

SUBSTRATE OPTIMIZATION

A. Introduction to Raman Spectrometer

SERS technique has become popular in a variety of fields because of its rapid detection and specific structural information. However, its reproducibility poses significant challenges, with scientists reporting difficulties in reproducing other researchers' experiments.[70-71] This is due to several factors that could affect the fabrication of the substrate and the mixing, in turn affecting the final analyte-metal surface interactions.[70, 72] Recent studies in SERS have been investigating how different parameters could affect Raman enhancement. Better control of substrate formation and mixing will generate more reproducible analyte-metal surface interactions, which will lead to more reproducible peaks.[70-71]

Optimizing the mechanism of nanoparticles synthesis in SERS experiments is essential since selecting the right parameters allows for control over the reaction's outcome.[52] However, the choice of synthetic route is not always trivial considering that nucleation and growth mechanisms of nanoparticles do not always follow classical models and is still under debate.[35, 52, 73] Therefore, it is generally accepted that investigating system parameters is a fundamental step in SERS experiments to obtain optimum responses.[51-52] Experimental assessment of parameters affecting nanoparticle formation like temperature,[52] time of reaction,[51] the role of reducing

agent[35, 51] and stirring[74] have been studied. Moreover, factors that affect analyte-metal surface interaction, such as pH[75], aggregating agent[76] and mixing technique[77] have also been investigated.

Figure 12 illustrates the steps involved in the experiment and the parameters to be optimized in each stage. First, the nanoparticles are synthesized according to the Lee and Meisel method, as described in Chapter 1. Second, they are mixed with an aggregating agent (NaCl) and the analyte of interest. The aggregating agent is important to aggregate nanoparticles and produce hotspots, which are zones of contact between the nanoparticles that enables high electromagnetic field enhancement.[35] Later, the sample is measured using a Raman detector. The parameters affecting Raman detection were discussed in Chapter 2.
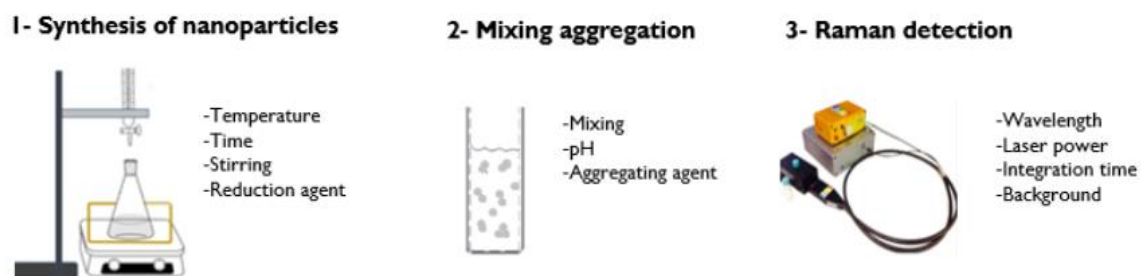
Figure 12. SERS protocol for nicotine detection and optimized parameters.

Table 3 shows the optimized parameters in this study. Reproducibility (triplicates during the same day) and repeatability (triplicates during different days) were investigated for every parameter, thus every optimal parameter was selected taking an average of nine measurements into consideration. Experimental procedures

and discussion of how every parameter affects the detection will be present later in this chapter.

Table 3: Substrate parameters optimized in this project.

Nanoparticle formation parameters	Parameters tested
Temperature of reaction	10, 50, 70, 92 and 97 °C
Time of reaction	10,20, 40, 60, 80 and 100 min
Rate addition of reducing agent	0.5, 1 and 2 drops per second
Stirring rate	200, 400 and 800 rpm
Mixing parameters	**Parameters tested**
Mixing method	Vortex and MIVM
Ph	3, 7 and 10
Concentration of aggregating agent	0, 0.1 and 1 M

B. Materials

Water (HPLC Grade) (CAS No 7732-18-5), was purchased from Fisher Chemical. Trisodium citrate (CAS No 6132-04-3) and Silver Nitrate (ACS Reagent, ≥99.0%) (CAS No 7761-88-8) from Sigma-Aldrich were used for the nanoparticle formation. For quantification, pure nicotine (CAS No 54-11-5) was procured from

Sigma-Aldrich. The aggregating agent used was Sodium Chloride (99.0%) (CAS No 7647-14-5) purchased from Himedia. To adjust the pH, Acetic Acid (100%) (CAS No 64-19-7) from Riedel-de Haen and Sodium Hydroxide (PA) (CAS No 1310-73-2) from Merck were purchased.

C. Substrate preparation method

The synthesis of the silver nanoparticles was adapted from the Lee and Meisel method; a reduction reaction between silver nitrate ($AgNO_3$) and sodium citrate ($Na_3C_6H_5O_7$).[53] Briefly, 0.018 g of $AgNO_3$ was added to a 100 ml of volumetric flask filled with 100 ml of HPLC grade water. The solution was transferred to an Erlenmeyer and the flask was heated in an oil bath at 280°C with constant stirring at 400 rpm too ensure homogeneous heating of the entire solution. Temperatures of the oil bath and the solution were controlled using digital thermometers. The tip of the thermometer was placed between the stirring bar and water surface to make sure the thermometer was fully immersed in the $AgNO_3$ solution. Two ml of 1% sodium citrate solution were added when the temperature of the solution reached 97 °C at the rate of one drop per second (manually added using a metronome set at 60 beats per minute). To make the 1 % sodium citrate solution, 0.5 g of sodium citrate was dissolved in 50 ml of HPLC grade water. After the addition of sodium citrate solution, the color of the solution changed from colorless to yellow and then milky gray. The reaction was then left for 80 minutes, while heating and stirring. Finally, the colloid

solution was left to cool down by stirring in a dark room to avoid the photodecomposition of silver. Characterization of the silver nanoparticles was done using DLS (dynamic light scattering) and UV/vis spectrometry (Ultraviolet–Visible spectrophotometer).

D. Acquisition of Spectra

Spectra of nicotine were obtained using a 785 nm portable Raman Spectrometry system (HR-TEC-X2 Stellar). Solutions of nicotine were prepared using HPLC grade water. The synthesized silver nanoparticles were mixed with an aggregate agent (NaCl 0.1 M) and nicotine solutions in a 9:1:1 mixing ratio. Then, the sample was vortex mixed for 1 minute and spectra were collected immediately after mixing, with an integration time of 10 seconds and laser power of 8. After the collection, peak areas were plotted and analyzed using Excel and Igor software.

E. Results and discussion

In this section, the optimization of the SERS parameters will be discussed separately. Collection of 9 samples (3 samples each day between 3 different days) were averaged to make a reasonable comparison between the parameters. Standard deviation (STD) and relative standard deviation (RSD) were calculated for triplicates of the same day (to assess reproducibility) and between different days (to assess repeatability).

1.Raman and SERS Spectra of nicotine

Nicotine is an amine composed of pyridine, which is a six-membered ring replaced by one nitrogen atom and a pyrrolidine ring (5-member ring).
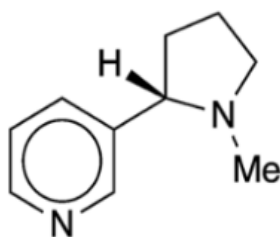
Figure 13. Nicotine molecule structure.

Initial measurements were taken to verify Raman peaks of nicotine and the detection limit of normal Raman spectra. Figure 14 shows Raman spectra of pure nicotine and the limit of detection of solutions of nicotine without the addition of nanoparticles.
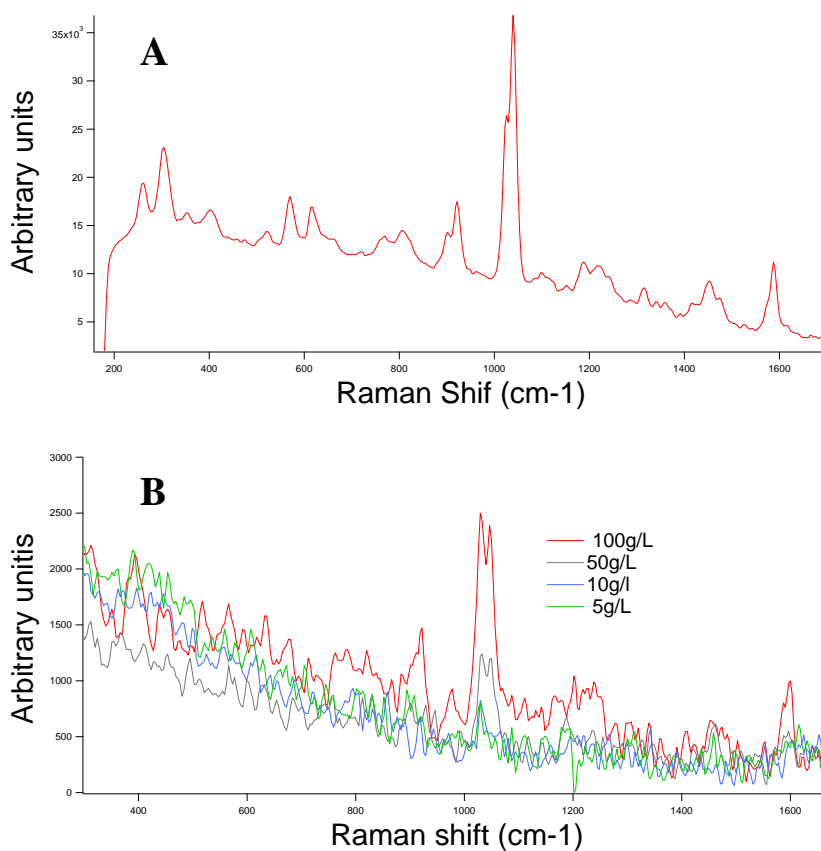
Figure 14. A) Spectra of pure nicotine, B) Limit of detection of solutions of nicotine.

The lowest normal Raman spectra detected was at 50000 ppm (50g/L), which proved the need for a surface enhancement to make the technique useful for our purpose. Figure 15 shows SERS Raman spectra of nicotine at 1 ppm, which shows an enhancement compared to Figure 14, where without the silver nanoparticles peaks from a solution of 50000 ppm could barely be identified. Figure 15 also presents several characteristic peaks at 1 ppm, increasing the detection by at least 5000 times.

Characteristic vibrations highlighted in Figure 15 are also reported in the literature, presented in Table 4.[29]
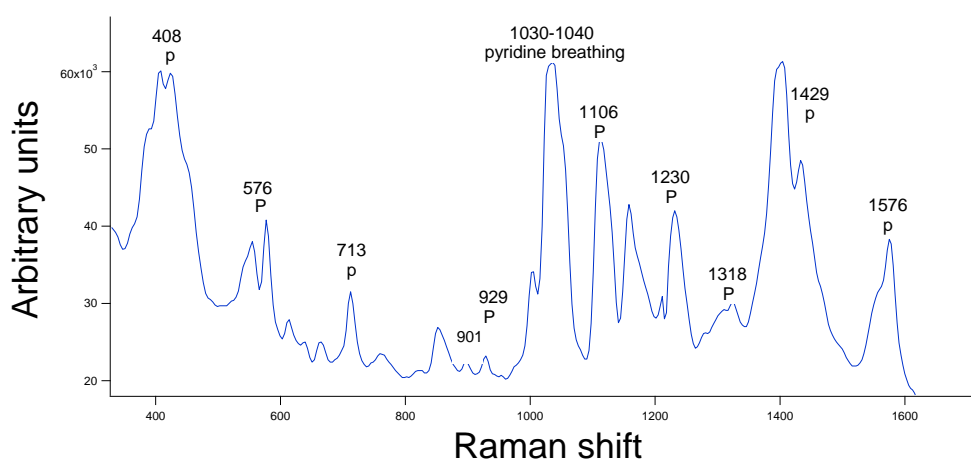
Figure 15. Nicotine SERS spectra at 1 ppm, with Raman vibrations identification, p represents pyridine vibration and P, pyrrolidine.

Table 4. Raman vibration peaks for nicotine reported in the literature.[29]

Raman peak (cm^{-1})	Vibration
408	Pyridine- out of plane ring deformation
573	Pyrrolidine- in plane ring deformation
713	Pyridine
925	Pyrrolidine – ring stretch
1030-1050	Pyridine – ring breathing
1105	Pyrrolidine- wagging
1227	Pyrrolidine- wagging

1318	Pyridine – twisting
1429	Pyridine – ring stretch
1578	Pyridine – ring stretch

Most of the papers detecting nicotine analyse the Raman vibration of 1030 cm$^-$^{1}.[28, 75-76, 78] This is because the spectrum of nicotine shows two main bands centred at 1032 and 1052 cm^{-1}, reported as being the symmetrical "breathing" and the trigonal deformation of the pyridine moiety respectively.[28-29] Nicotine approach the surface of silver nanoparticles through the pyridine ring rather than the pyrrolidine ring.[29, 75] Since pyridine ring adsorb in silver nanoparticles through the nitrogen atom, the enhancement is more apparent in this region, resulting in higher intensity peaks.[29]

2. Effect of temperature

Previous studies show that temperature is a crucial factor in nanoparticles synthesis involving sodium citrate, considering that sodium citrate requires relatively high temperatures due to its weak reducing strength.[79] It has also been reported that the reaction could be quenched at different stages by changing the temperature.[35, 51] Recently, it has been shown that the temperature change could change the reaction kinetics, the movement of atoms in the solution (Brownian motion) and the aggregative mechanisms of the nanoparticles.[80] This results in a change

in morphology, size and aggregation of the final product. As a result, peak enhancements also change.

Figure 16 shows SERS spectra collected with nanoparticles synthesized at different temperatures of 40, 50, 70, 92 and 97 °C. It is clearly noticeable from the color of the solutions that for our system, the reaction should be conducted at boiling temperatures, which coincides with the original Lee and Meisel method.[53] In addition, Figure 16B shows that solutions produced at temperatures of 40, 50 and 70 °C resulted in colorless solutions. Colloid solutions of silver nanoparticles are characterized as having a milky green-gray color, thus it can be assumed that at low temperature the silver colloid didn't form. This is also confirmed with the analysis of nicotine peaks, in which no peaks are presented. (Figure 16A)
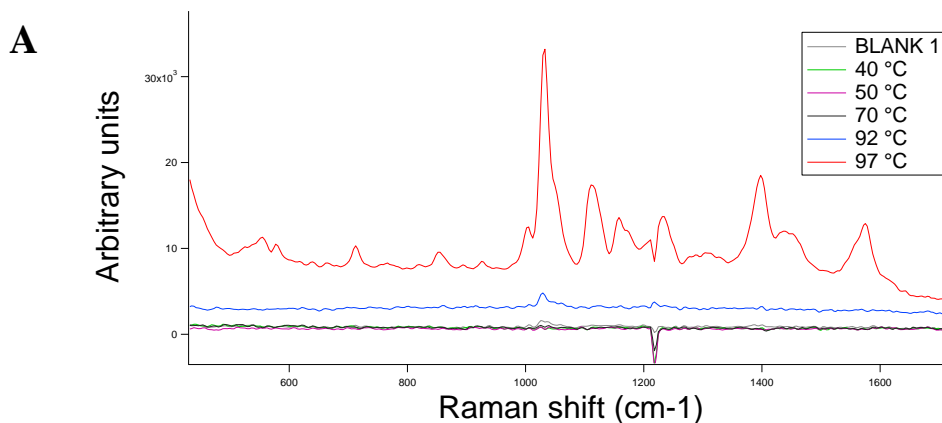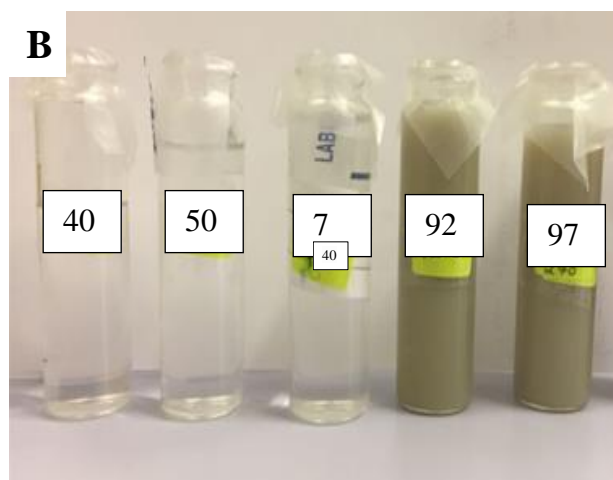
Figure 16.A) Effect of temperature in a synthesis of silver nanoparticles. The spectra show that a reaction at 97 °C produces better substrates for detection of nicotine. B) it is clearly noted that colloid nanoparticles are only formed after 92 °C.

3. Effect of reaction time

The reaction time has been reported as an important parameter for achieving complete reduction of silver.[51, 79] A study by Pillai et al show that, if the reaction is stopped after only 5-15 min of boiling, only partial reduction takes place.[51]

Figure 17 shows the effect of reaction time on the nicotine peaks in the SERS measurements. In the original Lee and Meisel method the reaction time was 60 minutes, but our results showed better spectra acquisition at 80 minutes, with an increase of 56.6% in peak area in comparison with 60 min (Table 5). In addition, we also tested reaction times of 10, 20, 40, and 100 minutes, with 10 and 20 minutes showing significantly smaller peaks, probably due to incomplete reduction as suggested in the literature.[51]
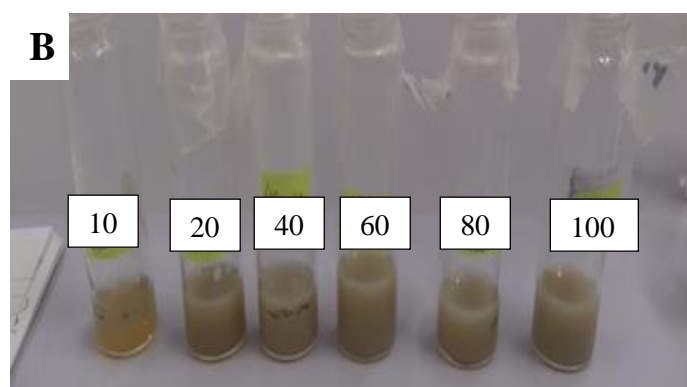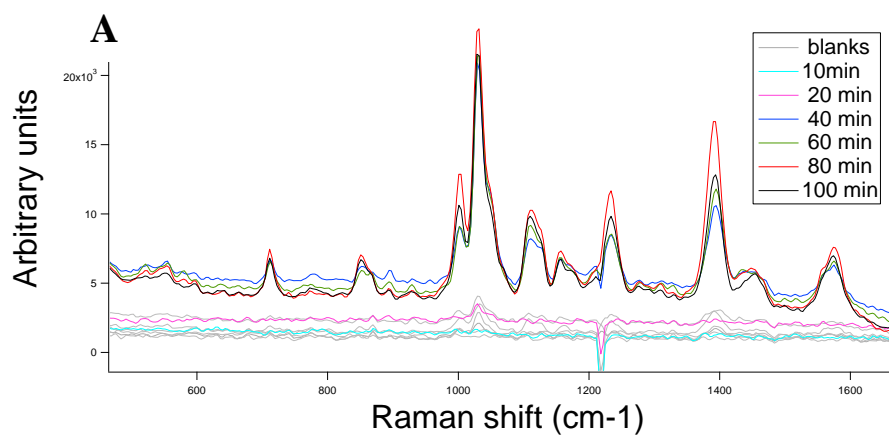
Figure 17.A) Effect of time on SERS spectra of nicotine, B) Aspect of different colloid solutions at different times. At 10 min, the solution is clear.

Table 5 – Peak areas of SERS nicotine spectra at different reaction times.

	60 min	**80 min**	**100 min**
DAY 1 AVERAGE	$3.23.10^5$	$5.38.10^5$	$5.59.10^5$
DAY 2 AVERAGE	$4.41.10^5$	$5.94.10^5$	$5.96.10^5$

DAY 3 AVERAGE	$4.45.10^5$	$7.61.10^5$	$4.97.10^5$
AVERAGE	$4.03.10^5$	$6.31.10^5$	$5.50.10^5$
STD	$5.67.10^4$	$9.50.10^4$	$4.08.10^4$
%RSD	14.07	15.05	7.42

4. Effect of Reducing agent

Sodium citrate plays an important role in the reaction, as highlighted in several studies.[51, 74, 81] A study by Pillai et al reported that increasing citrate concentration results in a greater amount of Ag^+ reduction.[51] It also mentioned that sodium citrate encourages the slow growth of silver particles, and it's concentration influences the reaction time to form the nanoparticles. Another study by Henglein and Giersig pointed out that low concentrations of citrate produce well separated small spherical particles. On the other hand, with a higher citrate concentration, clusters with broad size distribution are observed.[82] The mechanism of synthesis was explained, and the role of sodium citrate elucidated, in Chapter 1. Briefly, the citrate role is fundamental due to the formation of strongly complex with silver ions, and the local concentration of citrate affects the growth of nanoparticles by further aggregation.[51]

In this study, it was investigated how the rate of addition of sodium citrate affects the enhancement of SERS measurements at a fixed concentration of 1%, as reported by the original method of Lee and Meisel. Initial experiments were

conducted by adding sodium citrate with the use of a burette, without meticulous control of the addition. The addition using a burette was found to be inadequate, resulting in irreproducible spectra with low-intensity peaks as shown in Figure 18.
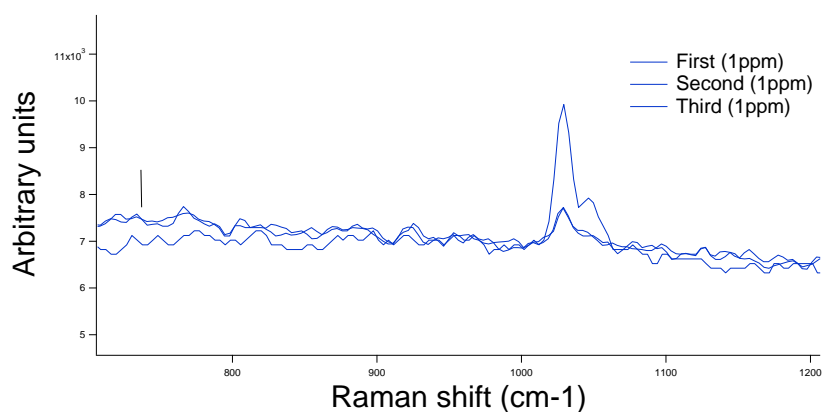
Figure 18. Triplicates of SERS nicotine spectra at concentration of 1ppm. The addition of sodium citrate using a burette produced irreproducible peaks with lower enhancement compared to controlled dropwise addition.

After concluding that a controlled addition would improve both reproducibility and peak enhancement, it was tested addition rates of 0.5, 1 and 2 drops per second. Figure 19 shows that the addition of 1 drop per second was optimal, resulting in more than double of peak area if compared with 0.5 and 2 drops per second (Table 6).
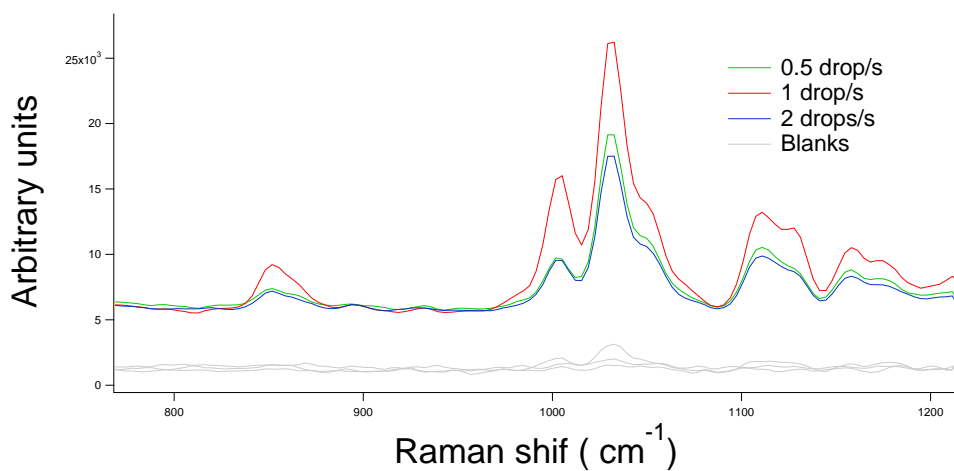
Figure 19. Nicotine SERS spectra with nanoparticles produced with the addition of 0.5, 1 and 2 drops per second. 1 drop per second showed to be optimal

Table 6. Peak areas of SERS nicotine spectra at different citrate rate addition.

	0.5 drop	1 drop	2 drops
DAY 1 AVERAGE	$2.92.10^5$	$7.73.10^5$	$2.49.10^5$
DAY 2 AVERAGE	$2.61.10^5$	$5.57.10^5$	$2.75.10^5$
DAY 3 AVERAGE	$3.11.10^5$	$6.09.10^5$	$2.62.10^5$
AVERAGE	$2.88.10^5$	$6.46.10^5$	$2.62.10^5$
STD	$2.08.10^4$	$9.21.10^4$	$1.06.10^4$
%RSD	7.22	14.25	4.04

44

5. *Effect of Stirring*

The stirring rate of the Lee and Meisel reaction was also reported to affect the substrate formation. A study by Munro et all showed that characteristic absorbance at the λ max was affected by changing stirring rates,[74] thus it can be assumed that this parameter also influences nanoparticle formation. Figure 20 shows the resulting spectra of substrates formed at 200, 400 and 800 rpm and it can be concluded that the peak height is not significantly affected by the stirring tare. The use of 200 rpm was excluded since the vortex formed in the solution wasn't completed. At 800 rpm, splashing was observed, and the peaks broadened, contributing to an increase in a peak area despite the unchanging peak height, as presented in the Table 7.

The optimal rate was found to be 400 rpm since the vortex reached the base of the stirrer and no splashing was observed.
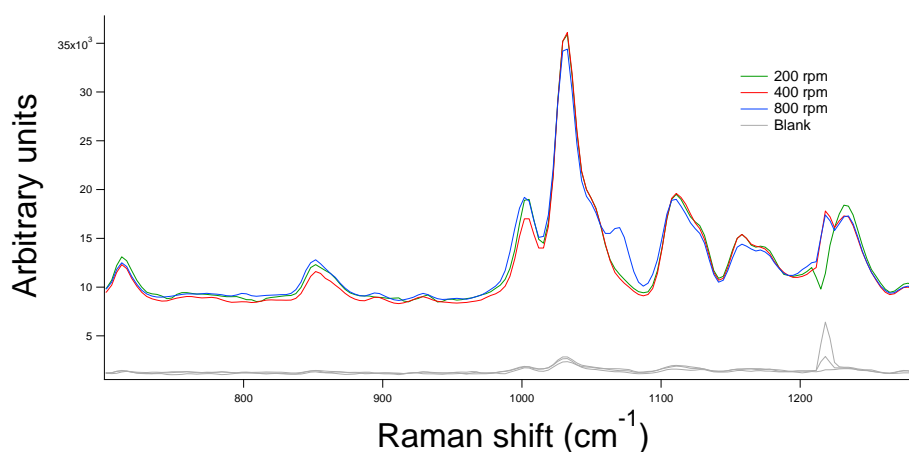
Figure 20. Nicotine SERS spectra with nanoparticles produced with stirring rates of 200, 400 and 800 rpm.

Table 7. Peak areas of SERS nicotine spectra at stirring rates.

	200rpm	400rpm	800rpm
DAY 1 AVERAGE	$8.20.10^5$	$6.89.10^5$	$9.04.10^5$
DAY 2 AVERAGE	$6.16.10^5$	$5.42.10^5$	$6.52.10^5$
DAY 3 AVERAGE	$6.49.10^5$	$8.30.10^5$	$8.52.10^5$
AVERAGE	$6.95.10^5$	$6.87.10^5$	$8.03.10^5$
STD	$8.92.10^4$	$1.18.10^5$	$1.09.10^5$
%RSD	12.84	17.12	13.52

6. Effect of mixing: MIVM and Vortex

Several studies aim to understand the colloid aggregation process during SERS measurements since it plays an essential role in controlling enhancement and reproducibility.[77] It has been reported that the final shape and size of metal clusters formed during aggregation will affect SERS enhancement. Freeman et al.[83] have highlighted the need to have better control over protocols during the formation of the SERS active clusters, considering that different SERS intensities are obtained from metal clusters of different effective diameter.

Two mixing techniques, the conventional Vortex and the Multi-Inlet Vortex Mixer (MIVM) were tested and compared. MIVM has been recently employed for the preparation of engineering materials at the nanoscale[84] and is mostly used to produce Flash Nano Precipitation (FNP) nanoparticles, a technique that was introduced by Johnson and Prud'homme in 2003.[85] In FNP, the size of the nanoparticles is controlled by the attachment of amphiphilic block copolymers onto the surface of the hydrophobic nanoparticle core. This technique has been used extensively in nanoscale drug delivery systems.[84]

In this study, MIVM was used to control the aggregation of nanoparticles by controlling the flow rates of addition of nanoparticles, aggregating agent (NaCl) and nicotine sample. Figure 21 shows MIVM the instrument, Harvard Apparatus 9000 Model, which consists of three syringe pumps and a multiple-inlet mixing chamber. Syringes containing the precursors have controlled flow rates, releasing the compounds automatically to the metallic mixing chamber.
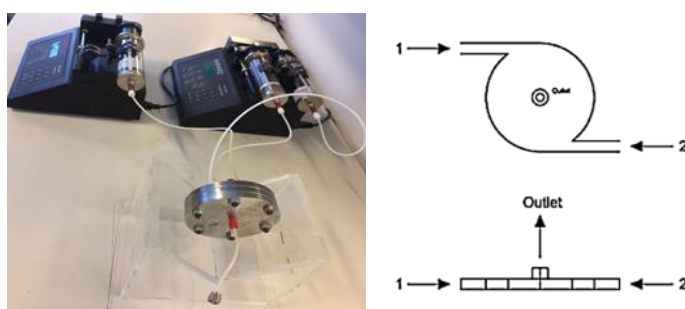
Figure 21. A Multi-Inlet Vortex Mixer (MIVM) equipment: at the top syringes contain the precursors which can be mixed with controlled flowrates and at the bottom the metallic mixing chamber and outlet. Right, representation of two-inlet MIVM top and side views.[84]

Since controlling mixing of FNP proved to result in a narrow, controlled size distribution of nanoparticles,[84] we wanted to test if the control of flow rates of nanoparticles, aggregating agent (NaCl), and nicotine would result in more reproducible or more enhanced spectra. The aim was to investigate if a homogenized mixing regime would provide nicotine chemisorption onto all available hotspots more uniform from run to run.

Figure 22 shows that MIVM provides better reproducibility for nicotine peaks at 10 ppm. Comparing graphs it can be noticed that MIVM established a more controlled mixing, which generates a decrease of sizes distribution of the aggregates of nanoparticles and nicotine. As a result, the reproducibility of aggregates MIVM and peak areas had improvement compared with the conventional vortex mixing.
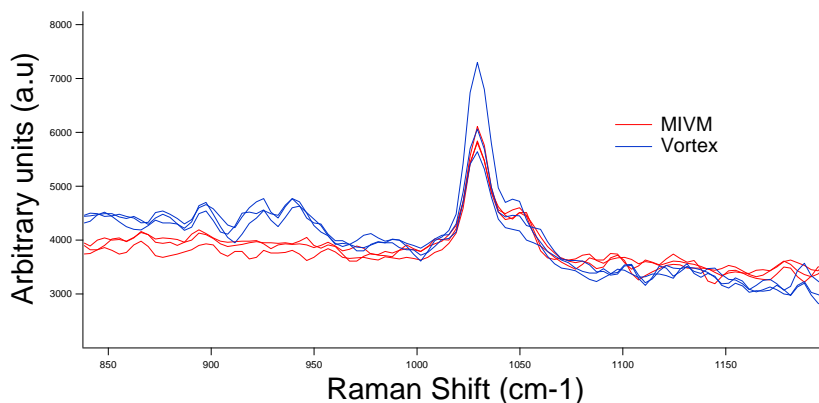
Figure 22. Nicotine SERS detection at 10 ppm Vortex mixing and MIVM mixing. Reproducibility showed to improve with MIVM technique.

Comparison was also made at lower concentrations of nicotine (1ppm). Figure 23 shows the use of vortex and MIVM have no significant difference in the final spectra.
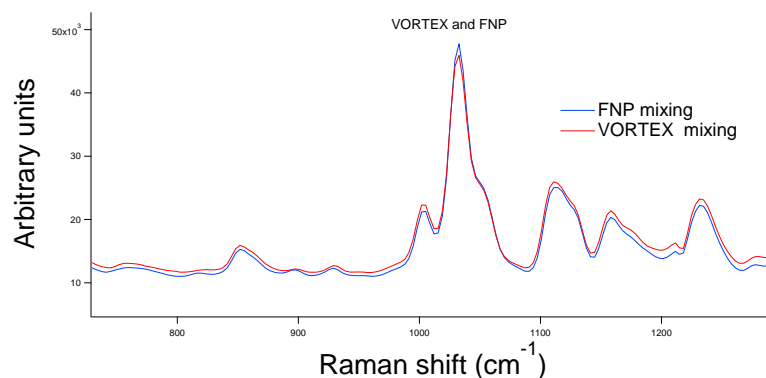
Figure 23. Comparison between Vortex and MIVM at 1 ppm. Graph represent average of 9 measurements (triplicates in three different days).

Another experiment tested if different flow rates would interfere in the enhancement, since MVIM allows for the adjustment of precursors flowrates. We tested if slow, medium or fast mixing would provide more reproducibility or better enhancement than the vortex mixing method. Figure 24 shows three different flowrate setups compared with a vortex. It can be noticed that the slow flow rate (1 ml/min, 9 ml/min) had a very high percentage error, probably because at slow flow rates the precursors did not mix properly. Set up 2 and 3 presented peak areas results similar to the vortex.

49

	Set up 1	Set up 2	Set up 3	VORTEX
NaCl	1ml/min	3ml/min	6ml/min	1
Nicotine	1ml/min	3ml/min	6ml/min	1
Silver Nanoparticles	9ml/min	27ml/min	54ml/min	9
Average areas	$4.44.10^5$	$6.87.10^5$	$6.40.10^5$	$6.37.10^5$
RSD	19.82	3.81	16.18	10.73

NaCl 0.1 M

Nicotine 10ppm

Silver Nanoparticles
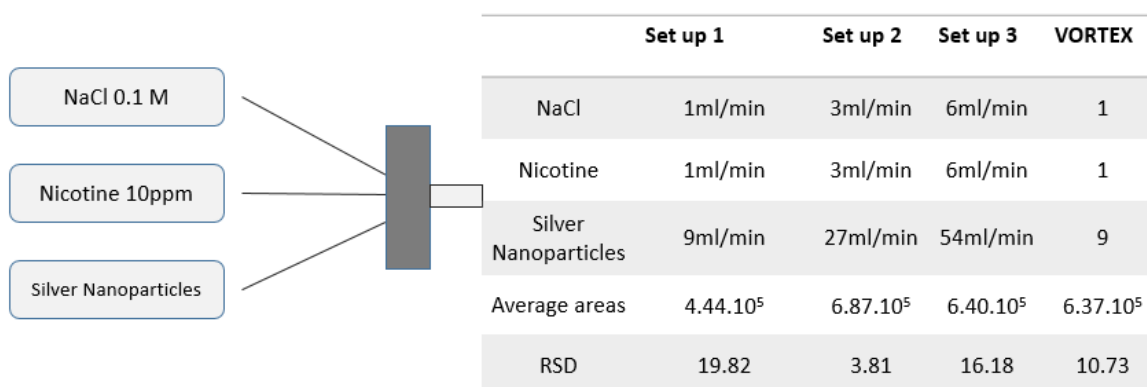
Figure 24. Peak areas of SERS nicotine spectra mixed with three different flowrates with MIVM and vortex.

Since the MIVM technique showed no significant improvement to our results, the study proceeded with the use of regular vortex. Previous Studies on SERS show the importance of mixing,[77, 86] and the literature suggests that data reproducibility can be improved by optimizing vortex time during colloid aggregation,[77] which was attributed to the formation of more reproducible metal clusters under conditions of 'forced convection`. In other words, optimizing the vortex time the effect of random collision is reduced (natural convection), due to fluid motion generated by an external source (forced convention).[77]

Figure 25 and Table 8 show the effect of vortex time on the final spectrum. With no vortex the peaks are smaller and the relative standard deviation (RSD) is higher than 20%, not being accepted as a reproducible result. This could be attributed to random collisions determining the creation of clusters. Figure 23 shows that the optimal time was one minute, with a significant improvement in RSD (from 41%, to

12%). At two minutes, the peak areas showed a decrease of 28% compared to one minute. This could be associated with the precipitation of some clusters, visually noticed as black points.
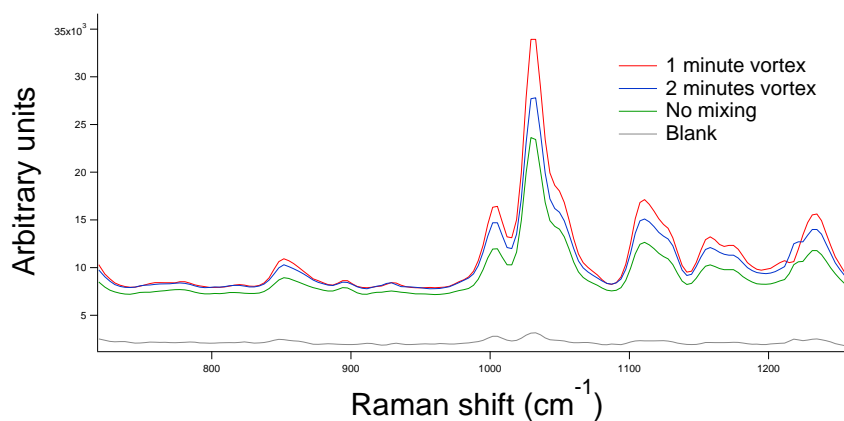
Figure 25. Nicotine SERS spectra mixed at several vortex times.

Table 8. Effect of vortex time on nicotine SERS spectra.

	0min	1min	2min
DAY 1 AVERAGE	$3.16.10^5$	$5.55.10^5$	$4.49.10^5$
DAY 2 AVERAGE	$2.54.10^5$	$4.41.10^5$	$3.15.10^5$
DAY 3 AVERAGE	$6.31.10^5$	$5.97.10^5$	$4.72.10^5$
AVERAGE	$4.01.10^5$	$5.31.10^5$	$4.12.10^5$
STD	$1.65.10^5$	$6.58.10^4$	$6.91.10^4$
%RSD	41.22	12.39	16.76

7. Effect of pH

Recent studies have examined the effects of pH on SERS measurements.[28, 75] pH affects the charge of the analyte of interest, affecting how the analyte would interact with the nanoparticle surface in turn.[35]

As the pH changes from acidic to alkaline, the conditions for the protonation of nicotine will be different, as shown in Figure 26.
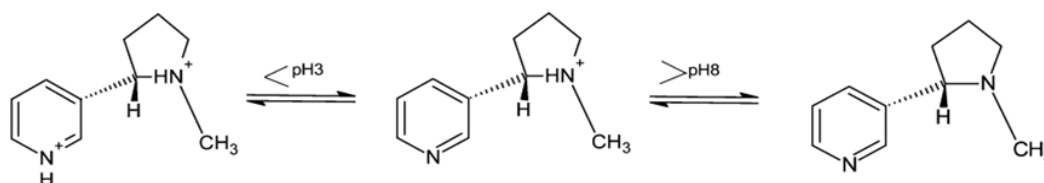
Figure 26. Ionization of nicotine in acidic and basic conditions.[75]

Nicotine has two pKa values: the first pKa is 3.12 for the pyridine ring and the second pKa is 8.02 for the pyrrolidine ring.[75] Both nitrogen atoms in the molecule have a lone pair of electrons that can be donated. Because of the resonance of the pyridine ring, the lone pair of electrons on the nitrogen of the pyridine ring is less readily available for protonation than the lone pair on the nitrogen of the pyrrolidine ring.[29, 75]

The pH of the medium highly influenced our measurements as shown in Figure 27. when the nicotine is protonated at low pH, the enhancement is significantly higher than at neutral or basic pH. Also, neutral pH showed to have irreproducible results. Nicotine spectra show that the maximum peak area is obtained at around pH 3, in

accordance with the literature.[28, 75] Comparing the peak areas, acidic medium demonstrated one order of magnitude increase compared to other pHs. Therefore, the protonation of pyridine is fundamental to ensure that the molecule will strongly interact with the silver nanoparticle due to electrostatic attraction.
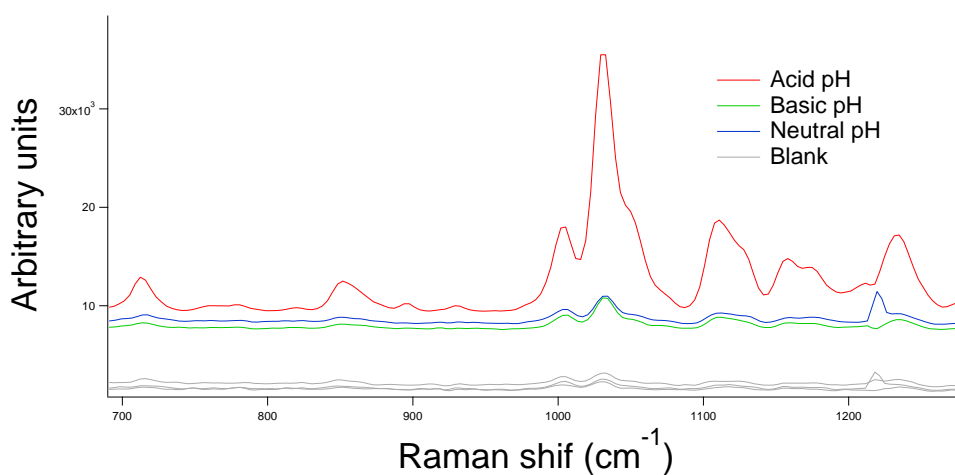
Figure 27. Effect of pH on SERS nicotine spectra.

Table 9. Effect of pH on SERS nicotine spectra.

	Acid pH (3)	**Neutral pH (7)**	**Basic pH (10)**
DAY 1 AVERAGE	$5.55.10^5$	$8.25.10^4$	$8.96.10^4$
DAY 2 AVERAGE	$4.41.10^5$	$3.49.10^4$	$9.07.10^4$
DAY 3 AVERAGE	$5.97.10^5$	$1.58.10^5$	$1.04.10^5$
AVERAGE	$5.31.10^5$	$9.17.10^4$	$9.47.10^4$

STD	$6.58.10^4$	$5.06.10^4$	$6.43.10^3$
%RSD	12.39	55.14	6.79

8.Effect of Aggregating agent

Aggregating agents added into the metallic colloid cause the nanoparticles to aggregate and create "hot spots" that generate high surface plasmon resonance.[35] the more hot spots created among the nanoparticles by aggregating agents, the higher the SERS enhancement.[49]

NaCl has been extensively used in SERS experiments as an aggregating agent.[28, 49, 75-76] Figure 28 shows the UV-Vis absorption spectrum of Ag colloidal solution with and without NaCl. UV/vis spectrometry is used to characterize colloid metal solutions since it can record absorption in the plasma resonance region. Without the aggregating agent, the maximum absorption for Ag colloidal solution was observed at 420 nm, in accordance with the literature.[53, 76] The addition of NaCl into the Ag colloidal solution leads to a decrease of absorption in the plasma resonance region. This phenomenon can be attributed to the aggregation of the nanoparticles.[76]
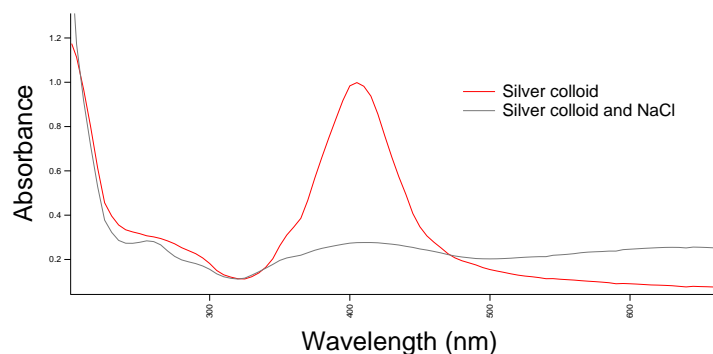
Figure 28. UV-Vis absorption spectrum of silver colloidal solution and aggregated colloidal solution. (with NaCl).

Figure 29 shows how different concentrations of NaCl influence the enhancement of nicotine. We can notice that with no addition of NaCl, no peak was detected, and theoretically, this could be explained by no creation of "hotspots". The optimal concentration was found to be 0.1 M, since at higher concentrations precipitation visually occurred. Table 11 shows DLS measurements with different salt concentrations. It can be noticed that at higher NaCl concentrations the nanoparticles agglomerate more.
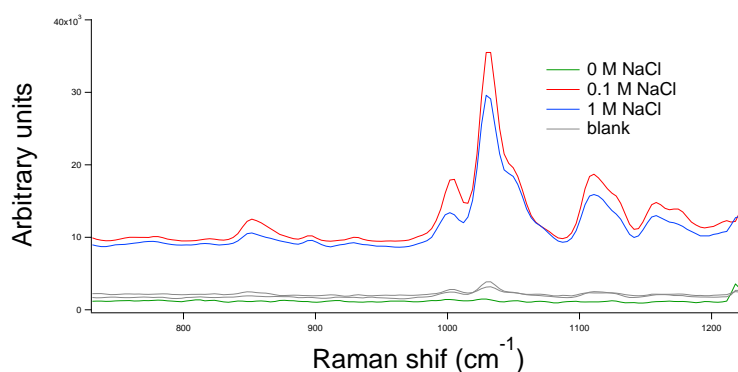
Figure 29. Effect of NaCl concentration on Nicotine SERS spectra.

Table 10. Effect of NaCl concentration on peak areas of Nicotine SERS spectra.

	No NaCl	0.1 M	1M
DAY 1 AVERAGE	0.00	$5.55.10^5$	$5.33.10^5$
DAY 2 AVERAGE	0.00	$4.41.10^5$	$3.75.10^5$
DAY 3 AVERAGE	0.00	$5.97.10^5$	$4.20.10^5$
AVERAGE	0.00	$5.31.10^5$	$4.43.10^5$
STD	0.00	$6.58.10^4$	$6.64.10^4$
%RSD	0.00	12.39	15.00

Table 11. Effect of NaCl concentration in diameter of aggregated silver nanoparticles.

Sample	Diameter (nm)
Silver Colloid	72.9
Silver Colloid with 0.1M NaCl (9:1)	74
Silver Colloid with 0.5M NaCl (9:1)	847.4

F. Conclusion

The present study was designed to determine how different parameters affect the SERS enhancement of nicotine by optimizing the conditions of the Lee and Meisel reaction. The most critical parameters in the fabrication of the substrate were found to

be temperature and time: at temperatures below the boiling point the peak areas dramatically decreased, and at short reaction times partial reduction would prevent a good spectral acquisition.

Moreover, mixing parameters showed to influence the analyte-metal surface interactions, consequently affecting the peak areas of nicotine. pH and aggregating agent concentration demonstrated to have an important role in SERS system with peak areas increasing one order of magnitude in acidic media. In addition, incorporation of NaCl as an aggregating agent had a major influence since no peak was detected without the addition of the salt.

CHAPTER 4

QUANTIFICATION OF NICOTINE IN URINE

A. Nicotine metabolism

The metabolism of nicotine is significantly complex and is influenced by several factors such as genetic factors, meals, age, sex, pregnancy, kidney disease, medications and smoking itself.[36] A full discussion of the pharmacokinetics of nicotine in the body lies beyond the scope of this study. However, it is important to understand the basics of nicotine metabolism.

After it has been absorbed by the body, nicotine is extensively metabolized to several metabolites by the liver. Six primary metabolites of nicotine have been recognized.[36] The major metabolite is cotinine, since about 70– 80% of nicotine is converted to cotinine. In addition, 10–15% of nicotine absorbed by smokers is discarded of in the urine as unchanged nicotine.[36, 87]

Nicotine measurement is highly specific for tobacco use or exposure, and its metabolism presents a short half-life of 2 h. Cotinine is also specific for tobacco use; however, the metabolism of cotinine is much slower than that of nicotine, with a long half-life of 16 h.[87]

B. Detection in biological samples

Nicotine and its metabolite cotinine can be detected in various biological samples, including urine, saliva, and blood.[36, 87] Thus, these compounds have been commonly used as biological markers to establish tobacco smoking status and estimate exposure to environmental tobacco smoke.[87-88]

Blood detection is considered an invasive method and the collection of samples is not simple, then it is preferred to opt for saliva and urine tests. As discussed in Chapter 1, concentrations in urine are around 10 times higher than saliva, with a range of 1 to 5 ppm in smokers. In addition, the collection of urine can be considered simpler than saliva, since in the protocol of saliva collection the subject has to refrain from eating, drinking, smoking or using oral hygiene products for at least 1 hour prior to collection.[89] On the other hand, urine samples can be collected directly without those limitations.

C. Matrix effect

A matrix effect is a change in the analytical signal caused by anything in the sample other than the analyte.[90] If a specific component can be identified as causing an effect then this is referred to as interference. Matrix effects have long been associated with bioanalytical samples and have to be considered to ensure that precision, selectivity, and sensitivity.[91]

The urine matrix could consist of a variety of compounds. About 91-96% of urine matrix consists of water.[92-93] The concentration of inorganic salts and organic compounds, including proteins, hormones, and a wide range of metabolites, varies from subject to subject. An average of these compounds is presented in Table 12.

Table 12. Compounds present in urine.[93]

Compound	Concentration
Water	91-96%
Chloride	1.87 g/L
Sodium	1.17 g/L
Potassium	0.750 g/L
Creatinine	0.670 g/L
Other (proteins, hormones metabolites)	variable

There are many strategies to minimize matrix effect such as sample dilution and optimization of sample preparation to remove interfering compounds.[90, 94] Sample dilution is only feasible when the sensitivity of the analysis is very high, which is not the case of this project. Optimizing sample preparation to remove interfering compounds from the samples is also mentioned as a good alternative to deal with matrix effect. Solid phase extraction (SPE) and liquid-liquid extraction are widely used as sample preparation techniques.[94] In addition, liquid-liquid extraction has the advantages of simple operation and apparatus. Charged compounds presented in urine matrix could also interfere with SERS measurements. Electrically charged species

naturally present in the urine could cause an undesirable formation of bigger particles, affecting the colloid stability.[28]

In this study, liquid-liquid extraction was employed to eliminate charged species and interferences and extract nicotine.

D. Liquid- liquid extraction

For the liquid-liquid extraction procedure, a method previously developed in our laboratory was adapted.[95]

Briefly, nicotine extracted from urine samples was spiked with known amounts of nicotine solutions. For selectivity, analyses of blank samples of the appropriate biological matrix of urine were obtained from at least six sources, in accordance with FDA guideline.[96] First, pH of the urine was set to basic (around 10) through the addition of 1M NaOH. Then 3 mL of toluene was added (Figure 28), and the mixture was shaken for 5 min. The mixture was then allowed to separate into toluene and aqueous phases. The toluene phase, which is capable of dissolving nicotine at a basic medium, was removed from the sample and then introduced into another vial containing acidic water. The pH was adjusted to 3 using 1M acetic acid. The change of pH leads to charged nicotine particles (as represented previously in Figure 25) which have a better affinity for the water phase. Figure 30 represents the schematic diagram of the extraction.
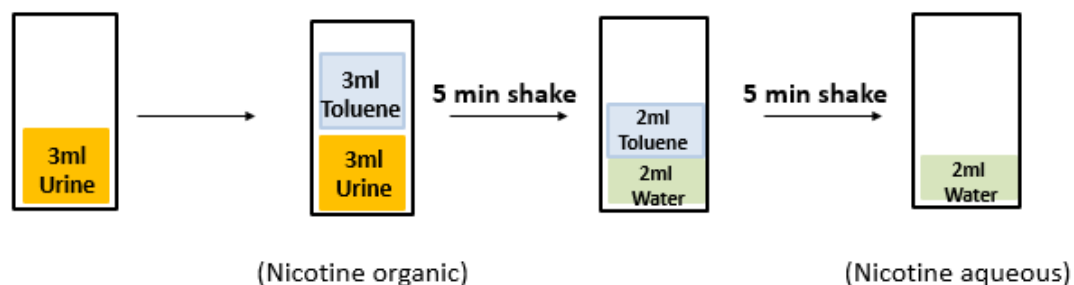
Figure 30. Schematic diagram for the extraction procedure adopted to separate Nicotine from urine.

E. Standard addition method

Most SERS studies have quantified target analytes in simple matrices (e.g. water) and when more complex backgrounds are involved, the task becomes more complex.[71] The charged and interfering species present in the matrix would compete with the nicotine particles for the metal NP surface needed for SERS, as mentioned before. As a result, the introduction of complex matrices affects the ability to perform accurate quantifications.[71, 97]

Standard addition method (SAM) for correcting matrix effects has been for any analyte in spectrophotometric analysis of biological fluids.[90] Recently, SAM has been used in experiments involving SERS detection.[28, 97-99] In brief, known quantities of the analyte are added to the unknown solutions. From the increase in the signals represented in the calibration curve, it can be deduced how much analyte was in the original unknown.[90]

As illustrated in Figure 31, SAM works by building a calibration curve from spiking known amounts of a standard into a sample of interest. From the calibration curve, the equation y=mx+b is generated, where m and b are the slope of the line and y-intercept, respectively. If the sample contains no analyte (nicotine standard) the intercept will be 0. However, when the sample contains the analyte the y-intercept will be positive. From these plots (upper plot in figure 29) the concentration of the analyte is determined from the extrapolation of the line at zero signal.[5]
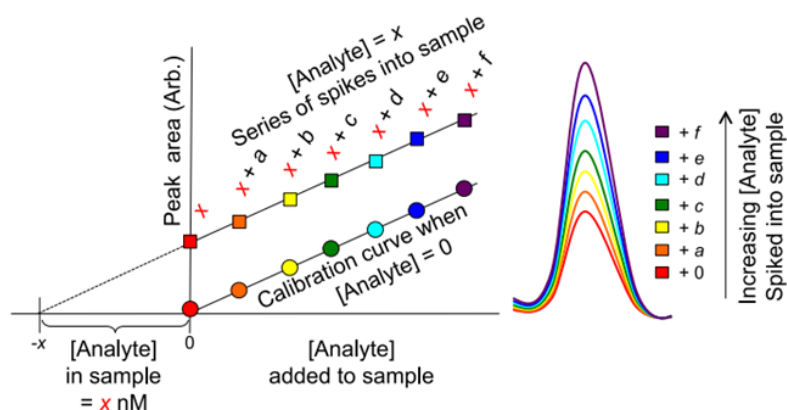
Figure 31. Representation of Standard addition method.[71]

The use of SAM in SERS experiments provide two main advantages: reduction in matrix effect and decrease in the significance of differences from one batch of nanoparticles to another.[97-98] This is because with SAM a new calibration curve is built in every measurement, therefore quantification can be done independently in each batch of nanoparticles.

63

In this study, liquid- liquid extraction in addition to Standard addition method were used. After liquid-liquid extraction of urine blank, known amounts of nicotine solutions from 1000ppm stock solution were added to different nanoparticles solutions, as shown in Figure 32.

Standards added to urine samples after liquid-liquid extraction

| 0 ppm | 1 ppm | 3 ppm | 5 ppm | 7 ppm | 10 ppm | 12 ppm |

100 μL nicotine solution
100 μL NaCl 0.1 M
900 μL silver nanoparticle
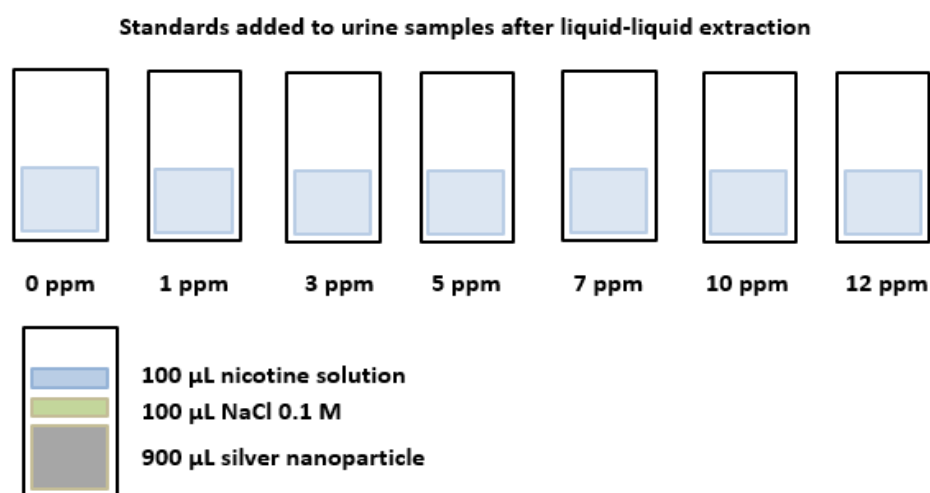
Figure 32. Standard addition method protocol for nicotine SERS detection in urine samples.

F. Results and discussion

1. Interference from cotinine

As mentioned previously, cotinine is the main metabolite of nicotine thus it is important to evaluate its interference. Figure 33 shows that the pyridine ring which presents the biggest contribution for the SERS spectra is present in both structures. This means that both molecules tend to approach the surface of silver nanoparticles

through the pyridine ring rather than the pyrrolidine ring, which can be attributed to the steric hindrance of the methyl group on the pyrrolidine ring.[100]
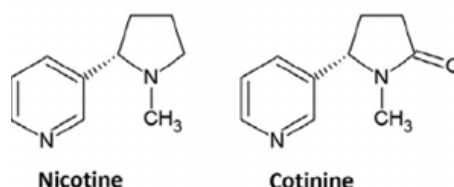
Figure 33. Structures of nicotine and cotinine.

Figure 34, 35 and 36 show spectra of nicotine and cotinine collected at different pHs: acidic (3), basic (10) and neutral (7). Nicotine detection is optimal in acidic media where cotinine interference is minimal. The pKa for the nitrogen within the pyridine ring being protonated is 3.12 in nicotine and 4.5 in cotinine is 4.5, which means that at a pH 3, both molecules will be protonated.[100] Nevertheless, the carbonyl group present in the cotinine molecule interferes with the adsorption geometry, resulting in a less pronounced pH effect. This could explain why the change of pH from neutral to acidic does not contribute significantly to the enhancement of cotinine peak.[100]
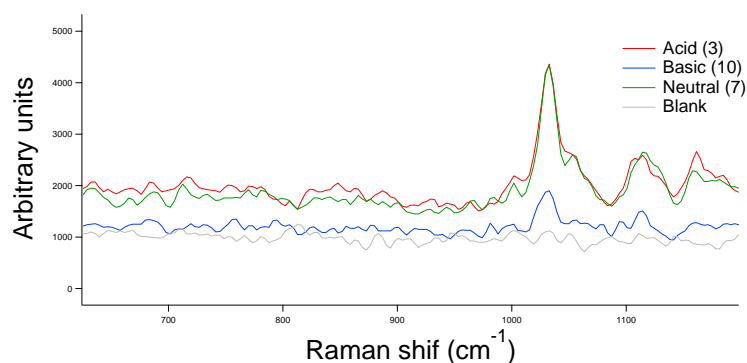
Figure 34. Cotinine SERS spectra at different pHs.

65
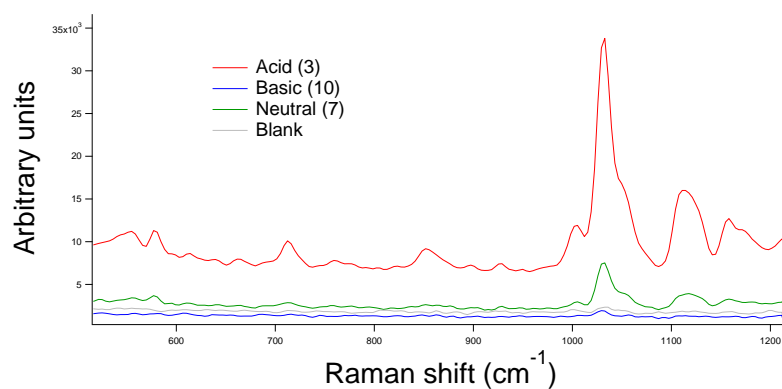
Figure 35. Nicotine SERS spectra at different pHs.
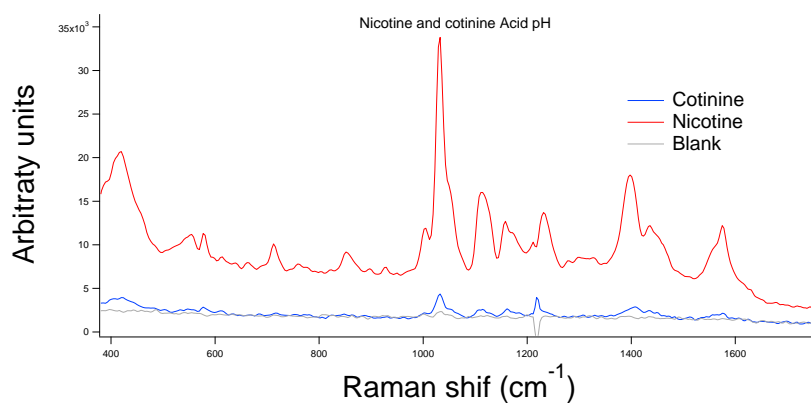
Figure 36. Nicotine and cotinine SERS spectra at acid pH.

.

2. Detection in biological samples

Figure 37 shows SERS spectrum in the urine system without any clean up (blue spectrum) and in water system (red spectrum), optimized in Chapter 3. This result confirmed the need for a clean-up method before detection since the matrix effect of urine samples hid all nicotine peaks.
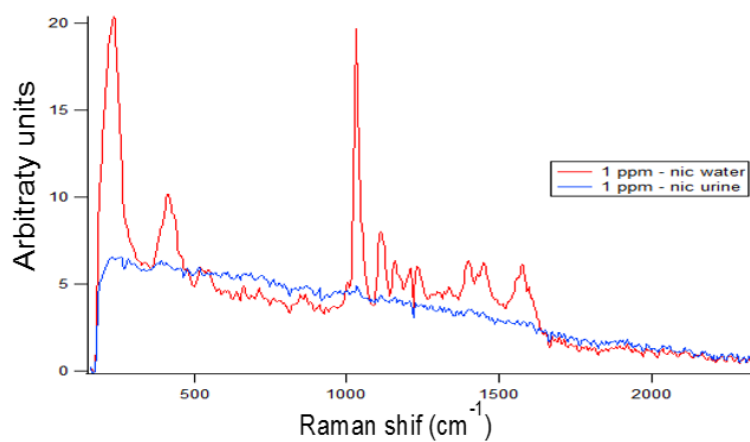
Figure 37. SERS spectrum in the urine system without any clean up (blue spectrum) and in water system (red spectrum).

Figure 38 shows the spectra of 1ppm spiked nicotine in urine after liquid-liquid extraction. the liquid-liquid extraction improved the detection by removing charged species and interferences from urine matrix
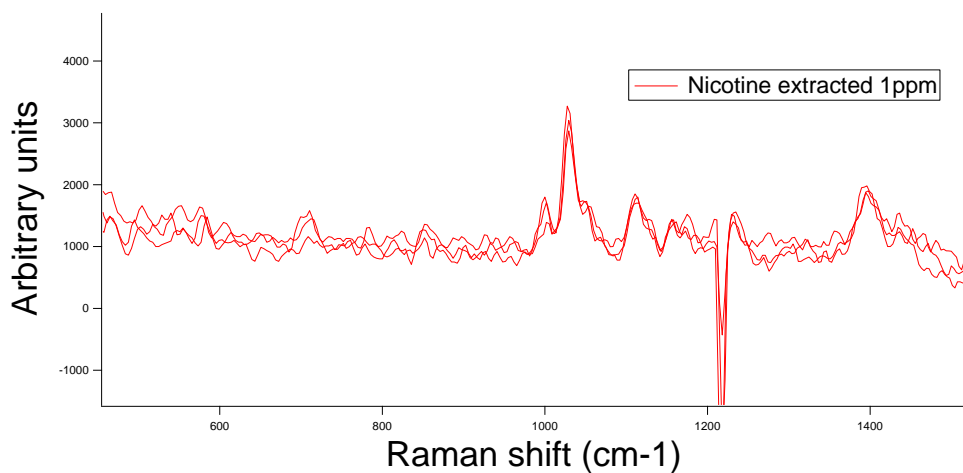
Figure 38. Nicotine SERS spectra from spiked urine sample detected after liquid-liquid extraction.

3. Standard addition method

Figure 39 and Table 13 show the results of SAM for quantification of nicotine in urine matrix. After liquid-liquid extraction, nicotine standards were added to the extracted solution. Each point was done in triplicates. As shown in Table 12, all relative standard deviation (%RSD) showed accepted values below 20%. Peak areas were plotted, and averages used to build a calibration curve. From the equation $y = 12918x + 14942$, the calculated concentration of the unknown was found to be 1.16, close to 1ppm of nicotine spiked before the liquid- liquid extraction.
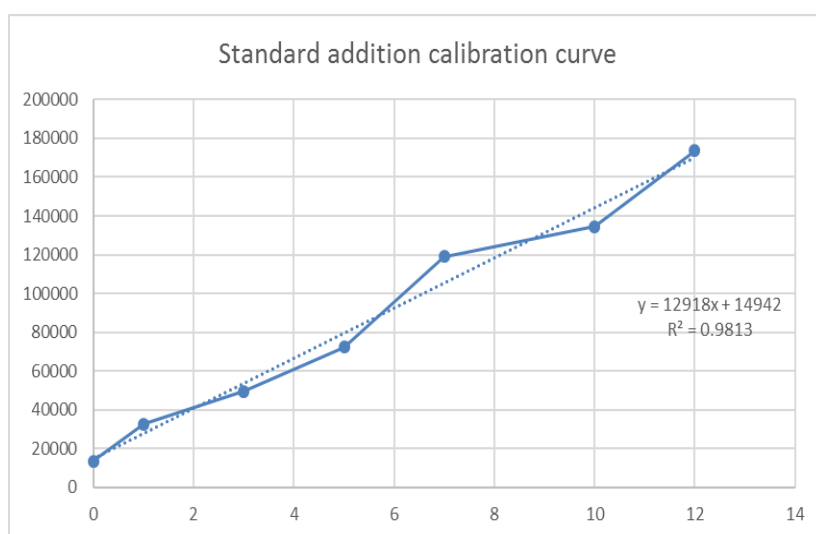
Figure 39. Standard addition calibration curve for nicotine detection in urine sample of 1ppm.

Table 13. Peak areas, STD and %RSD for standard addition method.

	BLANK	0	1ppm	3ppm	5ppm	7ppm	10ppm	12ppm
1	$1.33.10^4$	$2.79.10^4$	$4.16.10^4$	$5.15.10^4$	$7.15.10^4$	$1.08.10^5$	$1.63.10^5$	$1.85.10^5$
2	$9.57.10^3$	$2.32.10^4$	$3.65.10^4$	$6.73.10^4$	$1.04.10^5$	$1.43.10^5$	$1.43.10^5$	$1.95.10^5$
3	$8.43.10^3$	$2.13.10^4$	$5.15.10^4$	$6.13.10^4$	$7.31.10^4$	$1.38.10^5$	$1.28.10^5$	$1.73.10^5$
Average	$1.04.10^4$	$2.41.10^4$	$4.32.10^4$	$6.00.10^4$	$8.27.10^4$	$1.29.10^5$	$1.45.10^5$	$1.84.10^5$
STD	$2.10.10^3$	$2.76.10^3$	$6.25.10^3$	$6.50.10^3$	$1.48.10^4$	$1.56.10^4$	$1.44.10^4$	$8.98.10^3$
%RSD	20.07	11.46	14.47	10.83	17.87	12.09	9.95	4.88

E. Conclusion

In this Chapter the challenges of detecting nicotine in urine samples were discusses. Sample preparation was necessary since no peaks were detected in directly analysed urine samples. Liquid-liquid extraction showed to be an efficient method for extract nicotine from urine, cotinine, a major metabolite of nicotine, showed to have minimal interference at low ph. Finally, standard addition method provided considerably accurate results of quantification of nicotine.

CONCLUSIONS AND FUTURE WORK

Initially in this study, we highlighted the importance of nicotine detection in biological samples and SERS. Nicotine detection is important in clinical trials which have become essential to study not only exposure to toxicants but also to establish new products' regulations. Many techniques have been developed to test nicotine refrain. Recently surface enhanced Raman spectroscopy (SERS) has emerged as a potential technique providing a simple, rapid and low-cost method for nicotine detection.

In addition, the importance of parameters of Raman Spectrometer was demonstrated. Excitation wavelength showed to be a fundamental parameter to consider, since it is significantly related to higher sensitivity and decrease of fluorescence. Raman system parameters such as laser power and integration time were also significant parameters that affected the acquisition spectra. In some cases, only a small change of these parameters would duplicate the peak height. In addition, glass vials showed a significant interference in the spectra, and the system was customized to accommodate quartz vials, removing the background considerably.

Moreover, the optimization of the synthesis of silver nanoparticles was done. The most relevant parameters in the Lee and Meisel synthesis were found to be temperature and time. The optimal conditions were found to be 97 ° C and 80 minutes,

in which we got the best nanoparticles based on peak areas of nicotine SERS spectrum.

Mixing parameters of the nanoparticles with the analyte showed to influence the analyte - metal surface interaction, thus affecting the peak areas of nicotine spectrum. The pH and aggregating agent concentration conditions demonstrated to have an important role in SERS system. For example, in acid medium (pH = 3), peak areas increased one order of magnitude compared to basic medium. In addition, NaCl role as an aggregating agent had also major influence by forming "hot-stops", in which no peak was detected without the addition of the salt.

Finally, issues detecting nicotine in urine samples were discussed. Interference from cotinine, a major metabolite of nicotine, showed to be minimal at acid pH. Liquid-liquid extraction and standard addition method were used to overcome matrix effect. Liquid-liquid extraction showed to be an efficient method to extract nicotine and remove charged species from urine samples. Further, the standard addition method demonstrated to provide considerable accurate results for quantification of nicotine at low concentrations.

As a future work, the method should be validated by testing urine samples from smokers, non- smokers and subjects that abstain from nicotine for 12 hours. Application for the experiment was submitted to Institutional Review Board (IRB) six months ago, but the application are still under review. Hopefully, after approval the final step could be done for full validation of the method.

REFERENCES

1.   Lopez, A. D.; Murray, C. C., The global burden of disease, 1990–2020. *Nature medicine* **1998,** *4* (11), 1241.

2.   Organization, W. H., *WHO global report on trends in prevalence of tobacco smoking 2015*. World Health Organization: 2015.

3.   Baker, F.; Ainsworth, S. R.; Dye, J. T.; Crammer, C.; Thun, M. J.; Hoffmann, D.; Repace, J. L.; Henningfield, J. E.; Slade, J.; Pinney, J., Health risks associated with cigar smoking. *Jama* **2000,** *284* (6), 735-740.

4.   Peto, R.; Chen, Z. M.; Boreham, J., Tobacco—the growing epidemic. *Nature medicine* **1999,** *5* (1), 15.

5.   Bunnell, R. E.; Agaku, I. T.; Arrazola, R. A.; Apelberg, B. J.; Caraballo, R. S.; Corey, C. G.; Coleman, B. N.; Dube, S. R.; King, B. A., Intentions to smoke cigarettes among never-smoking US middle and high school electronic cigarette users: National Youth Tobacco Survey, 2011–2013. *Nicotine & Tobacco Research* **2015,** *17* (2), 228-235.

6.   Choi, K.; Forster, J. L., Beliefs and experimentation with electronic cigarettes: a prospective analysis among young adults. *American journal of preventive medicine* **2014,** *46* (2), 175-178.

7.   Primack, B. A.; Shensa, A.; Sidani, J. E.; Hoffman, B. L.; Soneji, S.; Sargent, J. D.; Hoffman, R. M.; Fine, M. J., Initiation of traditional cigarette smoking after electronic cigarette use among tobacco-naïve US young adults. *The American journal of medicine* **2018,** *131* (4), 443. e1-443. e9.

8.   Health, U. D. o.; Services, H., E-cigarette use among youth and young adults. A report of the Surgeon General. *Atlanta, GA: US Department of Health and Human Services, Centers for Disease Control and Prevention, National Center for Chronic Disease Prevention and Health Promotion, Office on Smoking and Health* **2016**.

9.   JUUL E-cigarettes Gain Popularity Among Youth, But Awareness of Nicotine Presence

Remains   Low.   https://truthinitiative.org/news/juul-e-cigarettes-gain-popularity-among-youth.

10.   Drummond, M. B.; Upson, D., Electronic cigarettes. Potential harms and benefits. *Annals of the American Thoracic Society* **2014,** *11* (2), 236-242.

11.   Malek, N.; Nakkash, R.; Talih, S.; Lotfi, T.; Salman, R.; Karaoghlanian, N.; El-Hage, R.; Saliba, N.; Eissenberg, T.; Shihadeh, A., A Transdisciplinary Approach to Understanding Characteristics of Electronic Cigarettes. *Tobacco Regulatory Science* **2018,** *4* (3), 47-72.

12.   McMillen, R.; Maduka, J.; Winickoff, J., Use of emerging tobacco products in the United States. *Journal of environmental and public health* **2012,** *2012*.

13.   Vansickel, A. R.; Cobb, C. O.; Weaver, M. F.; Eissenberg, T. E., A clinical laboratory model for evaluating the acute effects of electronic "cigarettes": nicotine delivery profile and cardiovascular and subjective effects. *Cancer Epidemiology and Prevention Biomarkers* **2010**, 1055-9965. EPI-10-0288.

14.   Zhu, S.-H.; Sun, J. Y.; Bonnevie, E.; Cummins, S. E.; Gamst, A.; Yin, L.; Lee, M., Four hundred and sixty brands of e-cigarettes and counting: implications for product regulation. *Tobacco control* **2014,** *23* (suppl 3), iii3-iii9.

15.   Hughes, J. R.; Keely, J. P.; Niaura, R. S.; Ossip-Klein, D. J.; Richmond, R. L.; Swan, G. E., Measures of abstinence in clinical trials: issues and recommendations. *Nicotine & Tobacco Research* **2003,** *5* (1), 13-25.

16.   Bullen, C.; McRobbie, H.; Thornley, S.; Glover, M.; Lin, R.; Laugesen, M., Effect of an electronic nicotine delivery device (e cigarette) on desire to smoke and withdrawal, user preferences and nicotine delivery: randomised cross-over trial. *Tobacco control* **2010,** *19* (2), 98-103.

17.   Møller, A. M.; Villebro, N.; Pedersen, T.; Tønnesen, H., Effect of preoperative smoking intervention on postoperative complications: a randomised clinical trial. *The Lancet* **2002,** *359* (9301), 114-117.

18.   Middleton, E. T.; Morice, A. H., Breath carbon monoxide as an indication of smoking habit. *Chest* **2000,** *117* (3), 758-763.

19.   Lichtenstein, E.; Grabowski, J.; Bell, C. S., Issues in the Measurement of Smoking: Summary and. *Measurement in the Analysis and Treatment of Smoking Behavior* **1983**, 105.

20.   Barlow, R. D.; Thompson, P. A., Simultaneous determination of nicotine, cotinine and five additional nicotine metabolites in the urine of smokers using pre-column derivatisation and high-performance liquid chromatography. *Journal of Chromatography B: Biomedical Sciences and Applications* **1987,** *419*, 375-380.

21.   Tuomi, T.; Johnsson, T.; Reijula, K., Analysis of nicotine, 3-hydroxycotinine, cotinine, and caffeine in urine of passive smokers by HPLC-tandem mass spectrometry. *Clinical chemistry* **1999,** *45* (12), 2164-2172.

22.   Man, C. N.; Gam, L.-H.; Ismail, S.; Lajis, R.; Awang, R., Simple, rapid and sensitive assay method for simultaneous quantification of urinary nicotine and cotinine using gas chromatography–mass spectrometry. *Journal of Chromatography B* **2006,** *844* (2), 322-327.

23.   Peeters, M.; Csipai, P.; Geerets, B.; Weustenraed, A.; van Grinsven, B.; Thoelen, R.; Gruber, J.; De Ceuninck, W.; Cleij, T.; Troost, F., Heat-transfer-based detection of L-nicotine, histamine, and serotonin using molecularly imprinted polymers as biomimetic receptors. *Analytical and bioanalytical chemistry* **2013,** *405* (20), 6453-6460.

24.   Alenus, J.; Ethirajan, A.; Horemans, F.; Weustenraed, A.; Csipai, P.; Gruber, J.; Peeters, M.; Cleij, T.; Wagner, P., Molecularly imprinted polymers as synthetic receptors for the QCM-D-based detection of l-nicotine in diluted saliva and urine samples. *Analytical and bioanalytical chemistry* **2013,** *405* (20), 6479-6487.

25.   Huynh, T.-P.; Chandra, B.; Sosnowska, M.; Sobczak, J. W.; Nesterov, V. N.; D'Souza, F.; Kutner, W., Nicotine molecularly imprinted polymer: Synergy of coordination and hydrogen bonding. *Biosensors and Bioelectronics* **2015,** *64*, 657-663.

26.   Gonzalez, J. M.; Foley, M. W.; Bieber, N. M.; Bourdelle, P. A.; Niedbala, R. S., Development of an ultrasensitive immunochromatography test to detect nicotine metabolites in oral fluids. *Analytical and bioanalytical chemistry* **2011,** *400* (10), 3655-3664.

27.   Abad, A.; Manclus, J. J.; March, C.; Montoya, A., Comparison of a monoclonal antibody-based enzyme-linked immunosorbent assay and gas chromatography for the determination of nicotine in cigarette smoke condensates. *Analytical chemistry* **1993,** *65* (22), 3227-3231.

28.   Mamián-López, M. B.; Poppi, R. J., Standard addition method applied to the urinary quantification of nicotine in the presence of cotinine and anabasine using surface enhanced Raman spectroscopy and multivariate curve resolution. *Analytica chimica acta* **2013,** *760*, 53-59.

29.   Barber, T. E.; List, M. S.; Haas, J. W.; Wachter, E. A., Determination of nicotine by surface-enhanced Raman scattering (SERS). *Applied spectroscopy* **1994,** *48* (11), 1423-1427.

30.   Jing, Y.; Yuan, X.; Yuan, Q.; He, K.; Liu, Y.; Lu, P.; Li, H.; Li, B.; Zhan, H.; Li, G., Determination of nicotine in tobacco products based on mussel-inspired reduced graphene oxide-supported gold nanoparticles. *Scientific reports* **2016,** *6*, 29230.

31.   Wu, N.; Luo, Z.; Ge, Y.; Guo, P.; Du, K.; Tang, W.; Du, W.; Zeng, A.; Chang, C.; Fu, Q., A novel surface molecularly imprinted polymer as the solid-phase extraction adsorbent for the selective determination of ampicillin sodium in milk and blood samples. *Journal of pharmaceutical analysis* **2016,** *6* (3), 157-164.

32.   Vashist, S. K.; Luong, J. H., *Handbook of Immunoassay Technologies: Approaches, Performances, and Applications*. Academic Press: 2018.

33.   Emmerich, G., Surface Plasmon Resonance: Technology Overview and Practical Applications.

34.   Prochazka, M., Basics of surface-enhanced raman scattering (SERS). In *Surface-Enhanced Raman Spectroscopy*, Springer: 2016; pp 21-59.

35.   Le Ru, E.; Etchegoin, P., *Principles of Surface-Enhanced Raman Spectroscopy: and related plasmonic effects*. Elsevier: 2008.

36.   Benowitz, N. L.; Hukkanen, J.; Jacob, P., Nicotine chemistry, metabolism, kinetics and biomarkers. In *Nicotine psychopharmacology*, Springer: 2009; pp 29-60.

37.   Kataoka, H.; Inoue, R.; Yagi, K.; Saito, K., Determination of nicotine, cotinine, and related alkaloids in human urine and saliva by automated in-tube solid-phase microextraction coupled with liquid chromatography–mass spectrometry. *Journal of pharmaceutical and biomedical analysis* **2009,** *49* (1), 108-114.

38.   Feyerabend, C.; Higenbottam, T.; Russell, M., Nicotine concentrations in urine and saliva of smokers and non-smokers. *Br Med J (Clin Res Ed)* **1982,** *284* (6321), 1002-1004.

39.   Jarvis, M.; Tunstall-Pedoe, H.; Feyerabend, C.; Vesey, C.; Salloojee, Y., Biochemical markers of smoke absorption and self reported exposure to passive smoking. *Journal of Epidemiology & Community Health* **1984,** *38* (4), 335-339.

40.   Shin, H.-S.; Kim, J.-G.; Shin, Y.-J.; Jee, S. H., Sensitive and simple method for the determination of nicotine and cotinine in human urine, plasma and saliva by gas chromatography–mass spectrometry. *Journal of Chromatography B* **2002,** *769* (1), 177-183.

41.	Moyer, T. P.; Charlson, J. R.; Enger, R. J.; Dale, L. C.; Ebbert, J. O.; Schroeder, D. R.; Hurt, R. D., Simultaneous analysis of nicotine, nicotine metabolites, and tobacco alkaloids in serum or urine by tandem mass spectrometry, with clinically relevant metabolic profiles. *Clinical chemistry* **2002,** *48* (9), 1460-1471.

42.	Colthup, N., *Introduction to infrared and Raman spectroscopy*. Elsevier: 2012.

43.	Comparison of Raman and IR Spectroscopy. http://www.chemvista.org/ramanIR4.html.

44.	Nakamoto, K., IR and Raman spectra of Inorganic and coordination Compound, part A and B. *Applications in Coordination, Organometallic and Bioinorganic Chemistry* **1998**, 60.

45.	McCreery, R. L., *Raman spectroscopy for chemical analysis*. John Wiley & Sons: 2005; Vol. 225.

46.	Speed, J. Tailoring plasmonic substrates for SERS. University of Southampton, 2011.

47.	Procházka, M., *Surface-Enhanced Raman Spectroscopy: Bioanalytical, Biomolecular and Medical Applications*. Springer: 2015.

48.	Fleischmann, M.; Hendra, P. J.; McQuillan, A. J., Raman spectra of pyridine adsorbed at a silver electrode. *Chemical Physics Letters* **1974,** *26* (2), 163-166.

49.	Han, S., Optimization of Aggregating agents and SERS Substrates for SERS detection of Cotinine and trans 3'-hydroxycotinine. **2015**.

50.	Willets, K. A.; Van Duyne, R. P., Localized surface plasmon resonance spectroscopy and sensing. *Annu. Rev. Phys. Chem.* **2007,** *58*, 267-297.

51.	Pillai, Z. S.; Kamat, P. V., What factors control the size and shape of silver nanoparticles in the citrate ion reduction method? *The Journal of Physical Chemistry B* **2004,** *108* (3), 945-951.

52.	Pacioni, N. L.; Borsarelli, C. D.; Rey, V.; Veglia, A. V., Synthetic routes for the preparation of silver nanoparticles. In *Silver nanoparticle applications*, Springer: 2015; pp 13-46.

53.	Lee, P.; Meisel, D., Adsorption and surface-enhanced Raman of dyes on silver and gold sols. *The Journal of Physical Chemistry* **1982,** *86* (17), 3391-3395.

54.   Kruszewski, S.; Cyrankiewicz, M., Aggregated silver sols as SERS substrates. *Acta Physica Polonica-Series A General Physics* **2012,** *121* (1), A68.

55.   Jain, S.; Hughes, A., Ostwald ripening and its application to precipitates and colloids in ionic crystals and glasses. *Journal of Materials Science* **1978,** *13* (8), 1611-1631.

56.   Discover 50 years of Raman innovation by HORIBA. https://www.horiba.com/en_en/50yearsraman/.

57.   Adar, F.; Delhaye, M.; DaSilva, E., Evolution of instrumentation for detection of the Raman effect as driven by available technologies and by developing applications. ACS Publications: 2007.

58.   Giri, M. A. D. I., Developing Portable Raman Spectroscopy Methods for Identification of Raw Materials Used in Pharmaceutical Development and Manufacturing. **2017**.

59. Raman Fiber Probes. http://www.horiba.com/scientific/products/osd/spectroscopy-solutions/modular-raman/raman-fiber-probes/.

60.   Alexander, R., Advantages of Raman Spectroscopy when Analyzing Materials Through Glass or Polymer Containers and in Aqueous Solution. *PerkinElmer Inc* **2008**.

61.   Gałuszka, A.; Migaszewski, Z. M.; Namieśnik, J., Moving your laboratories to the field–Advantages and limitations of the use of field portable instruments in environmental sample analysis. *Environmental research* **2015,** *140*, 593-603.

62.   Zarei, M., Portable biosensing devices for point-of-care diagnostics: Recent developments and applications. *TrAC Trends in Analytical Chemistry* **2017,** *91*, 26-41.

63.   Miles, R. B.; Lempert, W. R.; Forkey, J. N., Laser rayleigh scattering. *Measurement Science and Technology* **2001,** *12* (5), R33.

64.   Yang, S.; Akkus, O., Fluorescence Background Problem in Raman Spectroscopy: Is 1064 nm Excitation an Improvement of 785 nm? Wasatch Photonics: Report: 2013.

65.   Yang, S.; Li, B.; Slipchenko, M. N.; Akkus, A.; Singer, N. G.; Yeni, Y. N.; Akkus, O., Laser wavelength dependence of background fluorescence in Raman spectroscopic analysis of synovial fluid from symptomatic joints. *Journal of Raman Spectroscopy* **2013,** *44* (8), 1089-1095.

66.   Tuschel, D., Selecting an excitation wavelength for Raman spectroscopy. **2016**.

67.   Palonpon, A. F.; Ando, J.; Yamakoshi, H.; Dodo, K.; Sodeoka, M.; Kawata, S.; Fujita, K., Raman and SERS microscopy for molecular imaging of live cells. *Nature protocols* **2013,** *8* (4), 677.

68.   Handbook, B. P., : Therapeutics and Advanced Biophotonics. L e ng t h (m): 2016.

69.   Garcia, C. S.; Abedin, M. N.; Ismail, S.; Sharma, S. K.; Misra, A. K.; Sandford, S. P.; Elsayed-Ali, H. In *Design and build a compact Raman sensor for identification of chemical composition*, Sensors, and Command, Control, Communications, and Intelligence (C3I) Technologies for Homeland Security and Homeland Defense VII, International Society for Optics and Photonics: 2008; p 69430I.

70.   Fisk, H.; Westley, C.; Turner, N. J.; Goodacre, R., Achieving optimal SERS through enhanced experimental design. *Journal of Raman Spectroscopy* **2016,** *47* (1), 59-66.

71.   Goodacre, R.; Graham, D.; Faulds, K., Recent developments in quantitative SERS moving towards absolute quantification. *TrAC Trends in Analytical Chemistry* **2018**.

72.   Smith, W., Practical understanding and use of surface enhanced Raman scattering/surface enhanced resonance Raman scattering in chemical and biological analysis. *Chemical Society Reviews* **2008,** *37* (5), 955-964.

73.   Polte, J., Fundamental growth principles of colloidal metal nanoparticles–a new perspective. *CrystEngComm* **2015,** *17* (36), 6809-6830.

74.   Munro, C.; Smith, W.; Garner, M.; Clarkson, J.; White, P., Characterization of the surface of a citrate-reduced colloid optimized for use as a substrate for surface-enhanced resonance Raman scattering. *Langmuir* **1995,** *11* (10), 3712-3720.

75.   Alharbi, O.; Xu, Y.; Goodacre, R., Simultaneous multiplexed quantification of nicotine and its metabolites using surface enhanced Raman scattering. *Analyst* **2014,** *139* (19), 4820-4827.

76.   Han, S.; Hong, S.; Li, X., Effects of cations and anions as aggregating agents on SERS detection of cotinine (COT) and trans-3′ -hydroxycotinine (3HC). *Journal of colloid and interface science* **2013,** *410*, 74-80.

77.   Tantra, R.; Brown, R. J.; Milton, M. J., Strategy to improve the reproducibility of colloidal SERS. *Journal of Raman Spectroscopy: An International Journal for Original Work in all Aspects of Raman Spectroscopy, Including Higher Order Processes, and also Brillouin and Rayleigh Scattering* **2007,** *38* (11), 1469-1479.

78.   Itoh, N.; Bell, S. E., High dilution surface-enhanced Raman spectroscopy for rapid determination of nicotine in e-liquids for electronic cigarettes. *Analyst* **2017,** *142* (6), 994-998.

79.   Capek, I., *Noble Metal Nanoparticles: Preparation, Composite Nanostructures, Biodecoration and Collective Properties*. Springer: 2017.

80.   Piñero, S.; Camero, S.; Blanco, S. In *Silver nanoparticles: Influence of the temperature synthesis on the particles' morphology*, Journal of Physics: Conference Series, IOP Publishing: 2017; p 012020.

81.   Yaffe, N. R.; Ingram, A.; Graham, D.; Blanch, E. W., A multi‐component optimisation of experimental parameters for maximising SERS enhancements. *Journal of Raman Spectroscopy* **2010,** *41* (6), 618-623.

82.   Henglein, A.; Giersig, M., Formation of colloidal silver nanoparticles: capping action of citrate. *The Journal of Physical Chemistry B* **1999,** *103* (44), 9533-9539.

83.   Freeman, R. G.; Bright, R. M.; Hommer, M. B.; Natan, M. J., Size selection of colloidal gold aggregates by filtration: effect on surface‐enhanced Raman scattering intensities. *Journal of Raman spectroscopy* **1999,** *30* (8), 733-738.

84.   Saad, W. S.; Prud'homme, R. K., Principles of nanoparticle formation by flash nanoprecipitation. *Nano Today* **2016,** *11* (2), 212-227.

85.   Johnson, B. K.; Prud'homme, R. K., Flash nanoprecipitation of organic actives and block copolymers using a confined impinging jets mixer. *Australian Journal of Chemistry* **2003,** *56* (10), 1021-1024.

86.   Faulds, K.; Littleford, R. E.; Graham, D.; Dent, G.; Smith, W. E., Comparison of surface-enhanced resonance Raman scattering from unaggregated and aggregated nanoparticles. *Analytical chemistry* **2004,** *76* (3), 592-598.

87.   Benowitz, N. L.; Jacob III, P.; Ahijevych, K.; Jarvis, M. J.; Hall, S.; LeHouezec, J.; Hansson, A.; Lichtenstein, E.; Henningfield, J.; Tsoh, J., Biochemical verification of tobacco use and cessation. *Nicotine & Tobacco Research* **2002,** *4* (2).

88.   Shiffman, S.; Dunbar, M. S.; Benowitz, N. L., A comparison of nicotine biomarkers and smoking patterns in daily and non-daily smokers. *Cancer Epidemiology and Prevention Biomarkers* **2014**, cebp. 1014.2013.

89.   Navazesh, M., Methods for collecting saliva. *Annals of the New York Academy of Sciences* **1993,** *694* (1), 72-77.

90.   Harris, D. C., *Quantitative chemical analysis*. Macmillan: 2010.

91.   Health, U. D. o.; Services, H., Guidance for industry, bioanalytical method validation. *http://www. fda. gov/cder/guidance/index. htm* **2001**.

92.   Premasiri, W. R.; Clarke, R. H.; Womble, M. E., Urine analysis by laser Raman spectroscopy. *Lasers in Surgery and Medicine: The Official Journal of the American Society for Laser Medicine and Surgery* **2001,** *28* (4), 330-334.

93.   Rose, C.; Parker, A.; Jefferson, B.; Cartmell, E., The characterization of feces and urine: a review of the literature to inform advanced treatment technology. *Critical reviews in environmental science and technology* **2015,** *45* (17), 1827-1879.

94.   Chambers, E.; Wagrowski-Diehl, D. M.; Lu, Z.; Mazzeo, J. R., Systematic and comprehensive strategy for reducing matrix effects in LC/MS/MS analyses. *Journal of Chromatography B* **2007,** *852* (1-2), 22-34.

95.   El-Hellani, A.; El-Hage, R.; Baalbaki, R.; Salman, R.; Talih, S.; Shihadeh, A.; Saliba, N. A., Free-base and protonated nicotine in electronic cigarette liquids and aerosols. *Chemical research in toxicology* **2015,** *28* (8), 1532-1537.

96.   DHHS, U.; FDA, C., Guidance for industry: bioanalytical method validation. US Department of Health and Human Services. *Food and Drug Administration, Center for Drug Evaluation and Research (CDER), Center for Veterinary Medicine (CV)* **2001,** *2015*.

97.   Hidi, I. J.; Jahn, M.; Weber, K.; Bocklitz, T.; Pletz, M. W.; Cialla-May, D.; Popp, J., Lab-on-a-chip-surface enhanced Raman scattering combined with the standard addition method: toward the quantification of nitroxoline in spiked human urine samples. *Analytical chemistry* **2016,** *88* (18), 9173-9180.

98.   Westley, C.; Xu, Y.; Thilaganathan, B.; Carnell, A. J.; Turner, N. J.; Goodacre, R., Absolute quantification of uric acid in human urine using surface enhanced Raman scattering with the standard addition method. *Analytical chemistry* **2017,** *89* (4), 2472-2477.

99.   Villa, J. E.; Poppi, R. J., A portable SERS method for the determination of uric acid using a paper-based substrate and multivariate curve resolution. *Analyst* **2016,** *141* (6), 1966-1972.

100.   Huang, R.; Han, S.; Li, X. S., Detection of tobacco-related biomarkers in urine samples by surface-enhanced Raman spectroscopy coupled with thin-layer chromatography. *Analytical and bioanalytical chemistry* **2013,** *405* (21), 6815-6822.